森林総研研報 Bull. For. & For. Prod. Res. Inst. No. 368, 1994 65～107

Fuzzy Logic Control of a Knuckle Boom Crane for Forestry Machines

by

ASPLUND, Christer [1] and FUKUDA Akifumi [2]

Summary: This report describes a knuckle boom crane control system for forestry machines. The control system moves the crane tip in a desired direction, with a desired speed, using the reference from, e.g. a three dimensional joystick. But it also moves the crane tip the shortest way and as fast as possible from a starting point to a target point. Crane tip speed is limited by the size and rotational speed of the hydraulic pump and the maximum allowed controller output to the electro－proportional valves. The target position could be input by the operator pointing at the target and a sensor measuring that position or by an intelligent sensor which finds the position of trees. Here, the crane tip is only operated in two dimensions using the boom cylinder and arm cylinder of the crane.

The controller of the system is a Fuzzy Logic Controller (FLC). The report describes somewhat the fuzzy set theory which is the basis of the FLC and the characteristics of the fundamental FLC designed here. By experiments on a prototype knuckle boom crane it is shown that the FLC has a robust behavior, despite the non-linearities caused by the hydraulic system and the geometry of the crane design. It is also shown that the crane control system remains robust when a 440 kg weight is hanged from the crane tip. The orthogonal distance error from the reference line to the crane tip, due to controller error, is less than 3 cm and less than 5 cm when sensor error is included. The total error is considered to be small enough for use in forestry machines. The time used for the transfer of the crane tip from the starting point to the target point along the straight path between the two points is almost 30% longer than the time used when no restriction is set on the used path with equal maximum controller output, ±0.8 Volt, to the proportional valves. One drawback with the FLC is that it does not utilize the full control range of [－1,5；1.5] Volt because of stability problems. Some possible solutions are suggested.

Finally it is concluded that a FLC has advantages compared to conventional controllers and is a feasible technique for constructing a crane control system. The natural extension of this project is to include the rotation of the crane and the extension of the arm in order to move the crane tip in three dimensions.

Table of contents

Received February 2, 1994 技術－15 Forestry Technology Division－15

(1) Swedish University of Agricultural Sciences, Department of Operational Efficiency, Herrgårdsvagen 122, S-77698 Garpenberg, Sweden. (Guest reseracher of STA felloship, staying at Forest Technology Division during April 1, 1993 to November 30, 1993)
(2) Forest Technology Division

1 Introduction

It is a common fact that a forestry machine has a crane in order to manipulate the trees it is harvesting or transporting. In some countries, especially in Scandinavia, it is also becoming common that other forest operations are performed using the crane. A common type of crane structure is the knuckle boom crane which is shown in fig. 1.

A harvester is used, as it's name reveals, for harvesting trees in thinning operations and in final fellings. The harvester crane is equipped with a processor in the crane tip which fells the tree, delimbs it and cuts it into specified lengths and then leave the logs on the forest floor. A typical operational speed is 50–60 trees/hour. When a stand has been cleared or thinned, it is time for the forwarder to transport the logs to the landing site. The forwarder drive around the harvested area and pick up the logs and load them onto the forwarder. A skilled operator can drive the machine forward while he is loading the logs. When the forwarders load carrier is full, the forwarder is taken to the landing site where it unloads, again using the crane. The described operations are from Swedish forestry. The above implies that the operator spend much time operating the crane. In fact the operator spend so much time on operating the crane that many operators have trouble from aching neck and shoulders. Through the years the control levers have been improved from directly, mechanically, manipulation of the valves of the controlled hydraulic actuators to electrical joystick controls. However, the joysticks still control every actuator separately.

In the future the time for the operator to concentrate on operating the machine will decrease, due to new and more complicated tasks. The long trend in forestry is from monocultures toward forests with high biological diversity. Clear cuttings will disappear and final fellings also, to be replaced by selective cuttings. The new conditions will put new constraints on the operator in order to minimize the disturbance on the environment he is working in. The harvester operator's concentration will be more directed to which tree to select and planning of the final biological result. Hence, in order for the operator to achieve a good biological result while maintaining a high productivity with quality, he will need help to operate the machine and the crane.

2 Knuckle boom crane

2.1 General description

The experimental knuckle boom crane was constructed by FFPRI. It is quite a small crane with a maximum reach of 2.8 meters from the crane pillar in the horizontal plane. The crane is mounted on a radio controlled "base machine" which has four hydrostatically driven wheels and articulated steering. A picture of the machine is shown in fig. 1.

The knuckle boom crane consist of four rigid parts: the crane pillar; the boom; the arm; and the extender. The crane pillar is mounted with a revolving joint on to the base machine. A three dimensional orthogonal coordinate system is defined to have it's origin in the center of this joint. The X coordinate is defined to be parallel with the machine in direction to the front, Y is defined to go from the right to the left side of the machine, and Z is defined to be vertical directed upwards. Hence, the crane pillar is revolving around the Z axis. The boom is mounted to the crane pillar with a revolving joint in a plane orthogonal to the XY plane. The arm is mounted to the boom with a revolving joint in the same plane as for the boom. The extender, finally, is sliding inside the arm in the extension of the arm.

The crane has four actuators for moving the crane tip to a desired position. A rotational hydrostatic motor is used for rotating the crane pillar. A cylinder is used for changing the angle between the crane pillar and the boom. The angle between the arm and the boom is also controlled with a cylinder and so is the length of the extender. In appendix A is a schedule of the hydraulic system and facts about the used actuators.

The flow to the actuators are controlled through eight electro—proportional valves, two for each actuator. The solenoids of the valves are controlled with four 24 volt 100 Hz PWM signals. Relays are used to select one of the two valves for each actuator in order to control the direction of motion for the actuators. The PWM signals are output from four amplifiers (Daikin ZH-6-10), who set the current level of the PWM signals according to the input 0-5 volt DC signal. The DC signals are set by an IBM 486 personal computer through a 12 bit DA converter (Interface AZI-3302). The ON/OFF modes of the relays (Matsushita HLAP 5) are set by a 24 volt digital signal

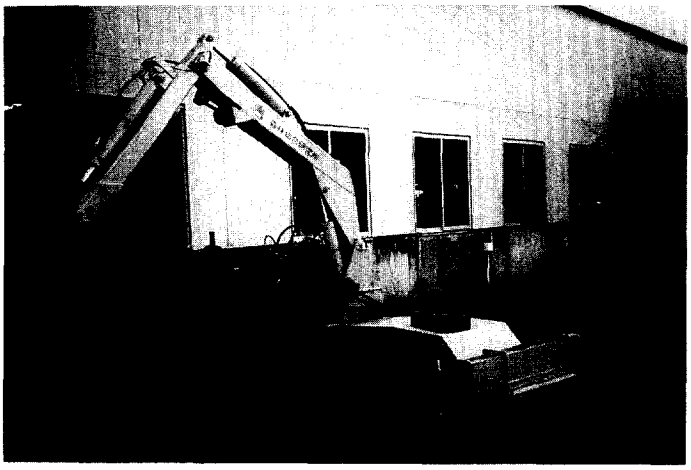

Fig. 1 Base machine and the knuckle boom crane

from a 16 channel PIO board (Contec PIO-16/16 (98)). The working range for the DC signals of the arm, boom and rotation actuator control is ± [1.7 ; 3.2] Volt and ± [1.7 ; 3.3] Volt for the extension cylinder control.

The crane is also equipped with four sensors. The rotation of the crane is measured using an incremental encoder and a 32 bit counter board (Interface AZI-818) which gives the resolution of 2 848 pulses/rad. The boom and arm angles are measured using rotational potentiometers, with the resolution of 2 409 bits/rad and 1 801 bits/rad respectively. The extender length is measured using a linear potentiometer, with the resolution of 10 578 bits/m, however the maximum extension is 0.37 m. The voltages from the potentiometers are read into the computer using a 12 bit AD converter (Contec AD 12-16 D (98)) with a conversion time of 1.56 μs. Some amplification of the potentiometer signals are made in order to adjust for the working range of each actuator. This will increase the resolution when the voltage signal is converted to a digital signal. A discussion on sensor accuracy can be found in appendix B.

2.2 Crane geometry

Up to this point a general description of the crane has been made. However, in this report only control of the boom and arm has been considered. Hence, the coordinate system has been redefined. Origin is defined to be in the joint between the crane pillar and the boom, and the boom and arm are defined to move in the XZ plane according to the illustration in fig. 2.

As mentioned in the previous section, the boom and arm angles are measured. From the measurements and geometry of the crane some other interesting variables can be calculated. Following are equations for calculation of crane tip position and speed, cylinder positions and speeds, and flow into each cylinder. More comprehensive calculations of the different equations can be found in the different appendixes. But first a more schematic drawing of the crane is shown in fig. 3.

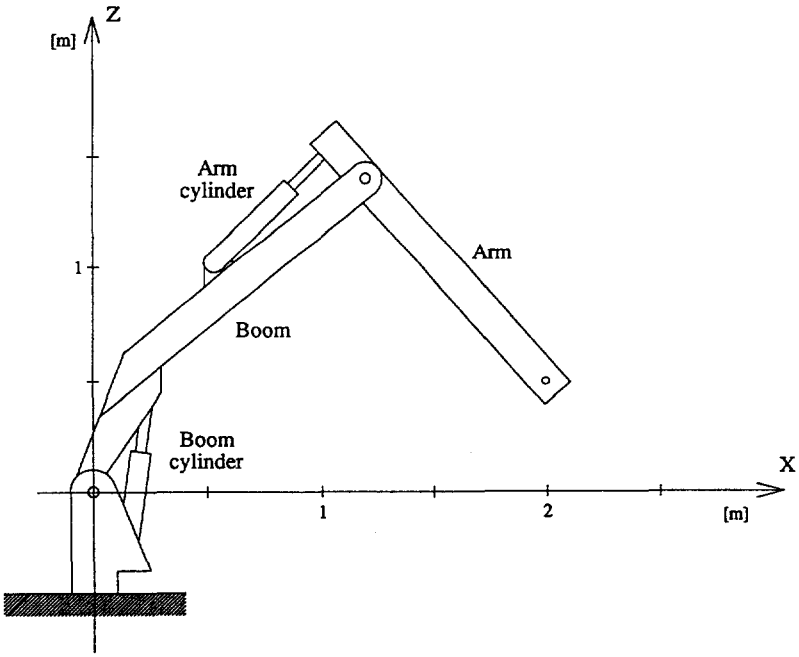

Fig. 2 Illustration of the two dimensional knuckle boom crane

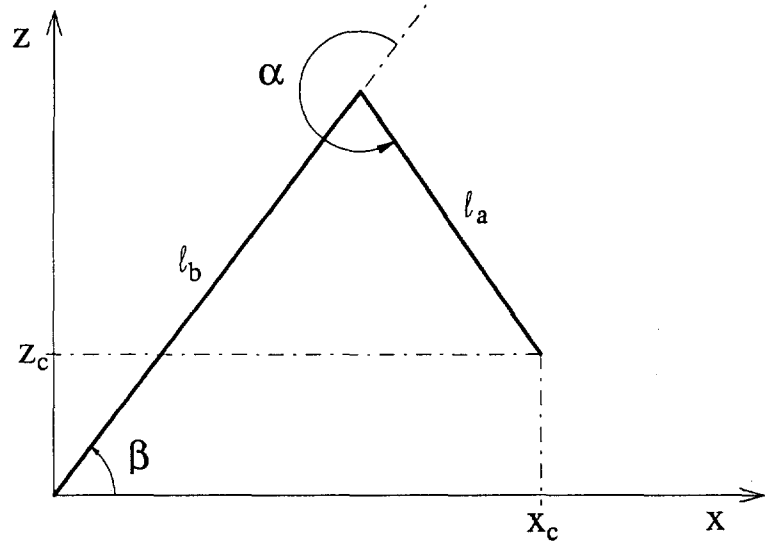

Fig. 3 Schematic drawing of the knuckle boom crane

From fig. 3 the position of the crane tip can be calculated using,

$$x_c(t) = l_b \cos\beta(t) + l_a \cos(\alpha(t) + \beta(t)) \tag{1}$$

$$z_c(t) = l_b \sin\beta(t) + l_a \sin(\alpha(t) + \beta(t)) \tag{2}$$

where

$x_c(t)$ is the crane tip position in X
$z_c(t)$ is the crane tip position in Z
l_a is the arm length
l_b is the boom length
$\alpha(t)$ is the arm angle
$\beta(t)$ is the boom angle

The inverse of (1) and (2) is,

$$\alpha(t) = \arccos\left(\frac{x_c(t)^2 + z_c(t)^2 - l_a^2 - l_b^2}{-2\, l_a l_b}\right) + \pi \tag{3}$$

$$\beta(t) = \arccos\left(\frac{l_a^2 - l_b^2 - x_c(t)^2 - z_c(t)^2}{-2\, l_b \sqrt{x_c(t)^2 + z_c(t)^2}}\right) + \arctan\left(\frac{z_c(t)}{x_c(t)}\right) \tag{4}$$

Since the arm and boom angles can only be within the ranges,

$\alpha \in [-2.533, -0.672]$ rad
$\beta \in [-0.058, 1.210]$ rad

The working area for the crane tip can be calculated using (1) and (2), which is shown in fig. 4. Crane tip speed can be calculated from the arm and boom angular speeds as,

$$\dot{x}_c(t)=g_1\cdot\dot{\alpha}(t)+g_2\cdot\dot{\beta}(t) \tag{5}$$

$$\dot{z}_c(t)=g_3\cdot\dot{\alpha}(t)+g_4\cdot\dot{\beta}(t) \tag{6}$$

where,

$$g_1=-l_a\sin(\alpha(t)+\beta(t)) \tag{7}$$

$$g_2=-l_b\sin\beta(t)-l_a\sin(\alpha(t)+\beta(t)) \tag{8}$$

$$g_3=l_a\cos(\alpha(t)+\beta(t)) \tag{9}$$

$$g_4=l_b\cos\beta(t)+l_a\cos(\alpha(t)+\beta(t)) \tag{10}$$

The inverse of equation (5) and (6) is,

$$\dot{\alpha}(t)=\frac{g_4}{g_1g_4-g_2g_3}\cdot\dot{x}_c(t)-\frac{g_2}{g_1g_4-g_2g_3}\cdot\dot{z}_c(t) \tag{11}$$

$$\dot{\beta}(t)=-\frac{g_3}{g_1g_4-g_2g_3}\cdot\dot{x}_c(t)+\frac{g_1}{g_1g_4-g_2g_3}\cdot\dot{z}_c(t) \tag{12}$$

Repeated in fig. 5a and 5b from appendix F are simple drawings of how the arm cylinder is mounted to the boom and arm, and how the boom cylinder is mounted to the crane pillar and boom. From fig. 5a and 5b the arm and boom cylinder lengths can be calculated according to,

$$x_a(t)=\sqrt{c_1+c_2\cos(\theta_1-\alpha(t))} \tag{13}$$

$$x_b(t)=\sqrt{c_3+c_4\cos(\theta_2-\beta(t))} \tag{14}$$

where c_1, c_2, c_3, c_4 and θ_1, θ_2 are constants calculated from k_1, k_2,...k_8 which can be found in appendix F.

The cylinder speeds as functions of the arm and boom angular speeds become,

$$\dot{x}_a(t)=\frac{c_2\sin(\theta_1-\alpha(t))}{2\sqrt{c_1+c_2\cos(\theta_1-\alpha(t))}}\dot{\alpha}(t) \tag{15}$$

$$\dot{x}_b(t)=-\frac{c_4\sin(\theta_2-\beta(t))}{2\sqrt{c_3+c_4\cos(\theta_2-\beta(t))}}\dot{\alpha}(t) \tag{16}$$

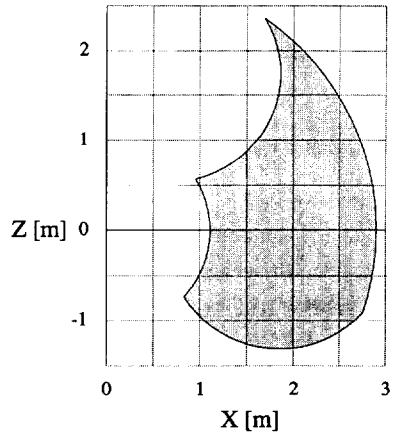

Fig. 4 Working area for the crane

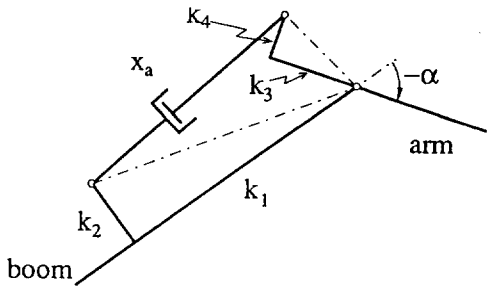

Fig. 5a Arm cylinder mounting between boom and arm

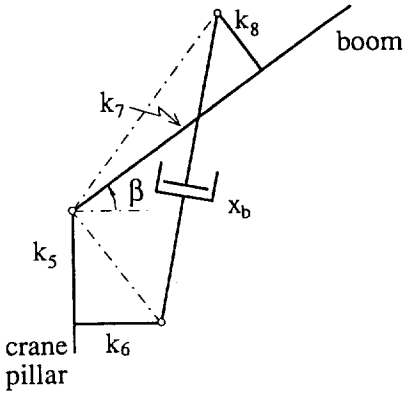

Fig. 5b Boom cylinder mounting between crane pillar and boom

But it is more interesting to know the hydraulic flow to each cylinder which is the cylinder area multiplied with the cylinder rod speed. However, the area is different for extension and contraction. The equations become,

$$\dot{P}_a(\dot{x}_a)=\begin{cases}\dfrac{\pi D_a^2}{4}\,\dot{x}_a, & \dot{x}_a\geqq 0\\ \dfrac{\pi\,(D_a^2-d_a^2)}{4}\,\dot{x}_a, & \dot{x}_a<0\end{cases} \tag{17}$$

$$\dot{P}_b(\dot{x}_b)=\begin{cases}\dfrac{\pi D_b^2}{4}\,\dot{x}_b, & \dot{x}_b\geqq 0\\ \dfrac{\pi\,(D_b^2-d_b^2)}{4}\,\dot{x}_b, & \dot{x}_b<0\end{cases} \tag{18}$$

Equation (17) and (18) implies that the hydraulic flow is positive when the cylinders are extending and negative when they are contracting. But, from the hydraulic system point of view, a flow is always required from the pump in order to change the position of the cylinder.

3 Crane control system

3.1 General control strategy

The geometry of a knuckle boom crane is quite similar to the geometry of many industrial robots, which implies that the control strategy also could be similar (SCHARF, 1985). Some examples can also be found where robotic techniques have been applied to knuckle boom cranes in order to simplify the operation (LÖFGREN, 1989 ; MOZUNA, 1992 ; UCHINO, 1993)

The aim of the control system is to move the crane tip from the current position in a requested direction or to a target position. The request or reference may come from the operator by using a joystick to input the direction or by using a pointing device in combination with a sensor to input the target position. But the target position could also come from a supervising control system which uses an intelligent sensor that for example locates the position of a tree.

The three dimensional joystick has three potentiometers, where the output signal from each potentiometer should correspond directly to the speed of the crane tip in three orthogonal coordinates. By integrating the three speed reference signals over time three position references in the three crane coordinates are obtained. The position reference should of course be calculated several times per second so the crane tip behave in the same way as the operator changes the joystick. When a target position is given as input it should be divided into subtargets, which correspond to positions where the crane tip should be, at different times. The path that the crane tip takes does not necessarily have to be the shortest one between the starting position and the target position. The sensor could for example give the position of obstacles, like stones or other trees, which the crane tip should avoid. The two different ways of giving the input results in position references where the crane tip should be at certain times.

When positioning the crane tip, it should move as fast as possible along the path decided by the supervising control system to the target position. The speed will be restricted by the available amount of hydraulic fluid from the pump and the maximum flow into the actuators. The maxi-

mum crane tip speed will change with the position of the crane tip and direction of motion. When using joystick control this maximum speed must be considered. The ordered speed from the joystick must never be higher than the maximum possible speed.

Additional requirements on the control system are that positioning should be within a couple of centimeters and that the crane tip should follow the given path within a couple of centimeters.

As mentioned in section 2.1 the measured variables are the arm and boom angles. The control variables are the two voltages to the electro−proportional valves, setting the flow to the arm and boom cylinders.

A straightforward way of controlling the crane tip, is to control the arm and boom angles. The arm and boom angle references are calculated using the inverse kinematics of the crane, which transform the crane tip reference position into arm and boom reference angles. The angle errors are formed by subtracting the reference angles from the measured angles, and these errors are fed into the angle controllers. The controllers calculate an output voltage for the electro−proportional valves (fig. 6). The calculations are made every 70 ms and so are the reference positions. How that is done will be treated in the next section.

3.2 Position reference calculation

When a target position, or as stated previously, a target path is given to the control system, the crane tip should follow the reference path as fast as possible. In order to do that, the maximum possible speed must be calculated at the current position in the requested direction. This speed can then be multiplied with the sample time which will be the change in reference position. The new reference position is then fed into the controller.

The maximum crane tip speed in X and Z directions is calculated using the fact that the relation between $\dot{x}_a(t)$ and $\dot{z}_c(t)$ is known and that the total hydraulic flow is limited. In fact even the flow to each cylinder is restricted. Hence,

$$C = \frac{\dot{z}_c(t)}{\dot{x}_c(t)} \tag{19}$$

$$P_{max} = |P_a(t)| + |P_b(t)|, \qquad |P_a(t)| \leqq P_{amax} \text{ and } |P_b(t)| \leqq P_{bmax} \tag{20}$$

Using (19) and (5), (6), (15) to (18), the relation between the flow to the arm cylinder and boom

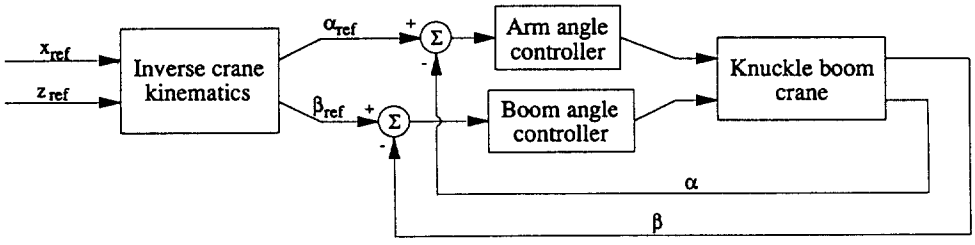

Fig. 6 The crane tip control system

cylinder can be calculated. With the flow relation and (20) the actual flow to each cylinder can be calculated. When the flow to each cylinder is known it is a simple task to calculate the crane tip speed. A more detailed calculation of the maximum possible crane tip speed can be found in appendix I. Observe that the maximum possible crane tip speed depends on the available amount of hydraulic flow, the current crane tip position and the requested direction of crane tip motion. Fig. 7 shows the maximum possible crane tip speed when the crane tip is moved in the positive direction along the X axis, and the hydraulic flow from the pump is limited to 38.9 ℓ/min and the maximum allowed flow to the arm and boom cylinders are 13.5 ℓ/min and 10.0 ℓ/min respectively.

By integrating the maximum possible crane tip speed a position reference can be obtained for the control system. However, since the crane tip will not be able to follow the reference position exactly and the exact maximum flows to the arm and boom cylinders, $Pa\max$ and $Pb\max$, are not known, but with some error, the speed will have to be multiplied with a factor. This factor has to be tuned with the actual crane.

Fig. 8 show calculation of the position reference. Here the aim is to move the crane tip as fast as possible in a requested direction, c. Maximum possible speed is calculated at the current crane tip position given by α (t) and β (t) in the requested direction c. The speed reference is multiplied with a factor k and integrated in order to get the reference position. The position reference is then fed into the controller according to fig. 6.

When a joystick is used it will give the reference speed. But the maximum possible speed is always calculated in order to limit the reference from the joystick according to fig. 9.

3.3 The fuzzy logic controller and theory

The controllers of the actuators could be any type of controllers, but here it was chosen to be Fuzzy Logic Controllers (FLC). Mainly because it is a technique which is becoming very popular and has shown good results when, for example, controlling an airplane (LARKIN, 1985), an industrial robot (SCHARF, 1985), a hydraulic cylinder (VIRVALO, 1992), and a subway train (YASUNOBU, 1983, 1985). The application described in this report was chosen because it is of interest for forestry but also because hydraulic systems often contains nonlinearities which makes control with conventional controllers more complicated.

The fuzzy set theory consist of several complex theorems, and is the basis of fuzzy logic control. The theory was first enunciated by Zadeh (ZADEH, 1973) and it's application in fuzzy logic control and terminology is comprehensively explained by, e.g. Lee (LEE, 1990a, 1990b). This section will define the used terminology and describe the fundamental properties of the theories behind the FLC in this application.

The structure of the FLC is shown in fig. 10. The inputs to the controller are the arm and boom angle errors, e_α and e_β, calculated according to fig. 6. However, the angle error changes which are equal to the angle speeds, s_α and s_β, must be calculated. This is done by subtracting the measured angle at the current sample with the measured angle four samples ago and then dividing with the time passed over the four samples. This algorithm will give a simple filtering effect, see appendix C.

The fuzzyfier performs a mapping that transfers the range of values of crisp input into corresponding universes of discourse. It also quantizes the inputs as shown in table 1, partly repeated here from table 1 in appendix J, in order to give the controller a more stable behavior as de-

scribed by (BOVERIE, 1991). Then the fuzzyfier performs the function of fuzzyfication which converts input data into the linguistic variables: arm angle error denoted as $E\alpha$; arm angle speed denoted as $S\alpha$; boom angle error denoted as $E\beta$; and boom angle speed denoted as $S\beta$, using information from the database.

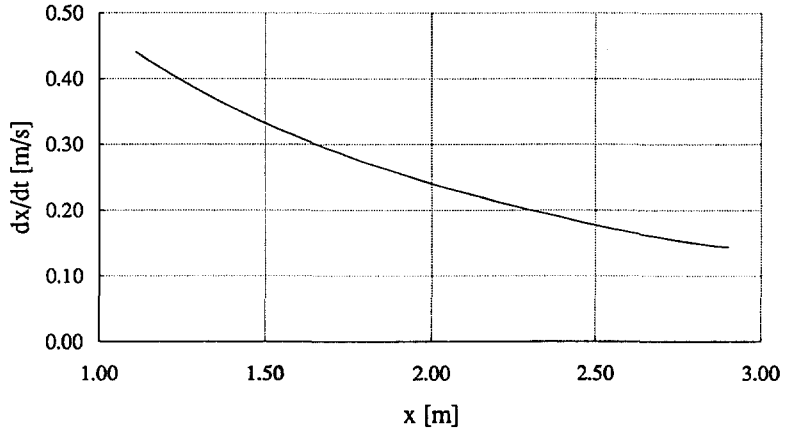

Fig. 7 Example of maximum possible crane tip speed when $z=0$

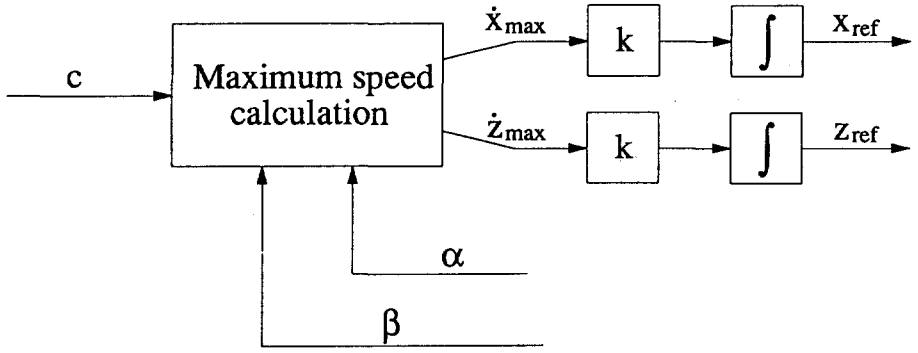

Fig. 8 Reference calculation for high crane tip speed

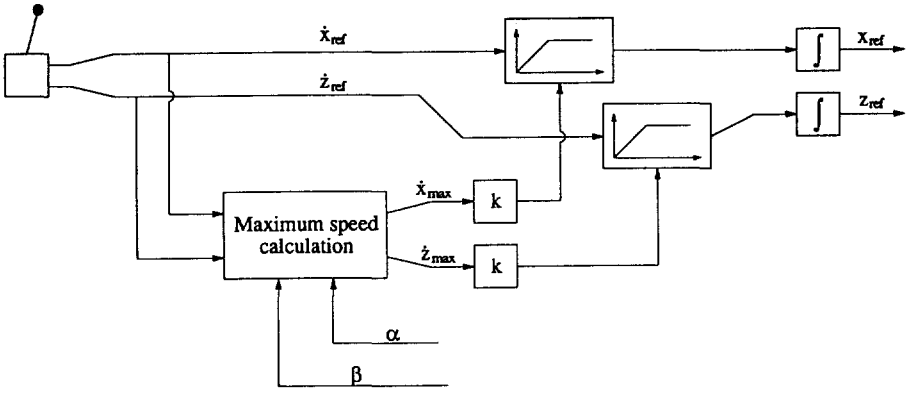

Fig. 9 Reference calculation when using joystick control

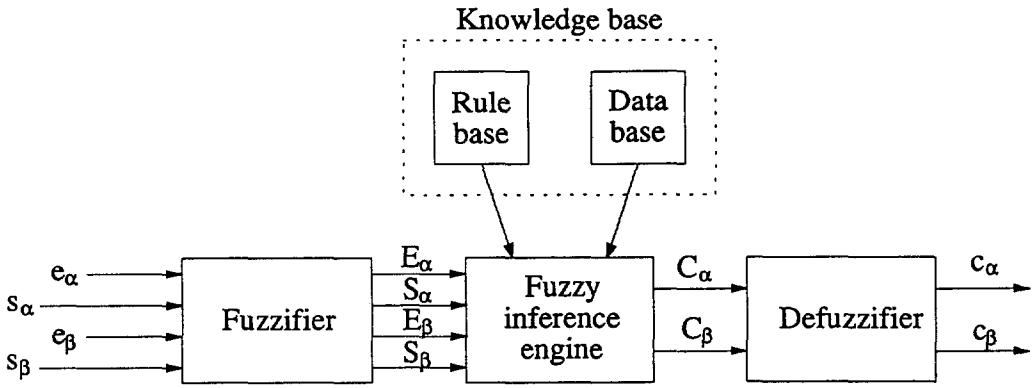

Fig. 10 Structure of the FLC

Table 1. Quantization of angle error.

Quantization level	Arm angle error, e_α [bit]	Boom angle error, e_β [bit]	Angle error [rad]	Quantized angle error [rad]
1	[91, 3 477]	[121, 3 177]	$-1.931 < e_\alpha \leqq -0.0500$ $-1.319 < e_\beta \leqq -0.0500$	-0.0500
2	[86, 90]	[115, 120]	$-0.0500 < e_\alpha, e_\beta \leqq -0.0475$	-0.0475
3	[82, 85]	[109, 114]	$-0.0475 < e_\alpha, e_\beta \leqq -0.0450$	-0.0450
⋮	⋮	⋮	⋮	⋮
20	[5, 9]	[7, 12]	$-0.0050 < e_\alpha, e_\beta \leqq -0.0025$	-0.0025
21	[−4, 4]	[−6, 6]	$-0.0025 < e_\alpha, e_\beta < 0.0025$	0.0000
22	[−9, −4]	[−12, −7]	$0.0025 \leqq e_\alpha, e_\beta < 0.0050$	0.0025
⋮	⋮	⋮	⋮	⋮
39	[−85, −82]	[−114, −109]	$0.0450 \leqq e_\alpha, e_\beta < 0.0475$	0.0450
40	[−90, −86]	[−120, −115]	$0.0475 \leqq e_\alpha, e_\beta < 0.0500$	0.0475
41	[−3 352, −91]	[−3 177, −121]	$0.0500 \leqq e_\alpha < 1.931$ $0.0500 \leqq e_\beta < 1.319$	0.0500

The value of a linguistic variable is a set of fuzzy sets. A fuzzy set A is defined in a universe of discourse U and characterized by a membership function $\mu_A(u)$ which assigns to each generic element $u \in U$ a number in the interval [0,1], which represents the degree of membership, namely, $\mu_A(u)$: $U \rightarrow [0,1]$. Thus a fuzzy set A in U may be represented as a set of ordered pairs of a generic element u and its membership function: $A = \{(u, \mu_A(u)) \mid u \in U\}$. In this application the membership functions are triangular in shape since computer calculations become efficient and since the shape of the function has little effect on the controllers behavior (BOVERIE 1991). Fig. 11 show the 11 fuzzy sets defined on the universe of discourse of angle error, and fig. 12 show the 9 fuzzy sets defined on the universe of discourse of angular speed. The names of the fuzzy sets are short for: P meaning positive; N meaning negative; ZE and Z meaning zero; S meaning small; M meaning medium; L meaning large; and EL meaning extra large. However, in the case of fuzzyfication, the crisp input is fuzzyfied into a fuzzy singleton, A', which has a membership function defined as $\mu_{A'}(u) = 1.0$ for $u = u_0$ and zero for all other u.

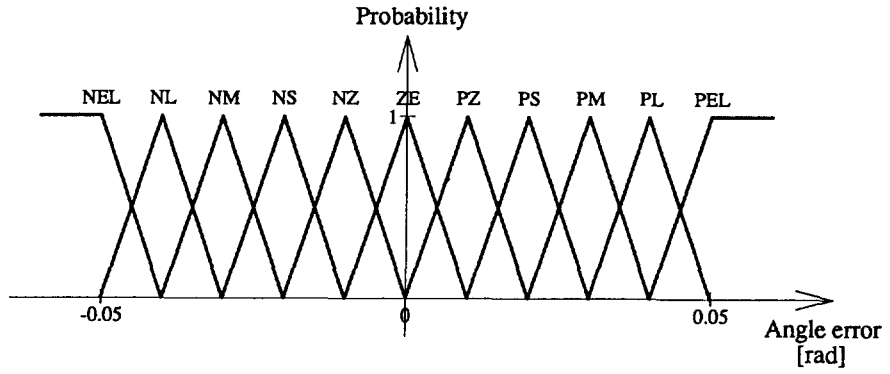

Fig. 11 Membership functions of the fuzzy sets defined to denote angle error

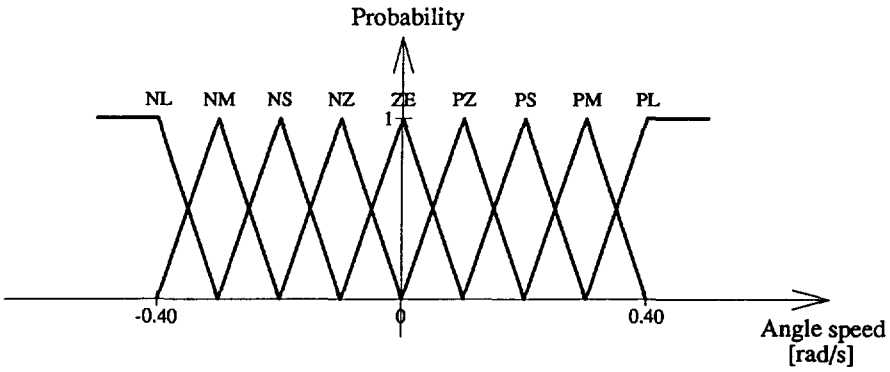

Fig. 12 Membership functions of the fuzzy sets defined to denote angle speed

The knowledge base comprises a knowledge of the application domain and the goals of the controller. It consists of a "rule base" and a "data base". The data base contain information on the quantization levels of crisp data and the definition of fuzzy sets and their respective membership function, as well as the universes of discourse. The rule base contain the fuzzy conditional statements, who characterizes the control goals.

A fuzzy conditional statement or fuzzy relation has the form of IF x is A AND y is B THEN z is C where A, B and C are fuzzy sets, and x, y and z are linguistic variables. x is A and y is B are the antecedents and z is C is the consequent. The dynamic behavior of the controller is characterized by a set of such fuzzy relations based on expert knowledge. The expert knowledge could come from a skilled operator of the system that is going to be controlled. In this application the antecedents are E_α and S_α, and the consequent is C_α, or the antecedents and consequent are E_β, S_β and C_β. The linguistic variables C_α and C_β represent the fuzzy value of the control action.

Fig. 13 shows a relation matrix which is a convenient way of representing many fuzzy relations. The entries of each row and column are the antecedents and the elements in the matrix are the consequent. The fuzzy relations represented by this relation matrix were developed by Virvalo and Koskinen (VIRVALO, 1992) and is used for the control of both the arm and boom cylinders.

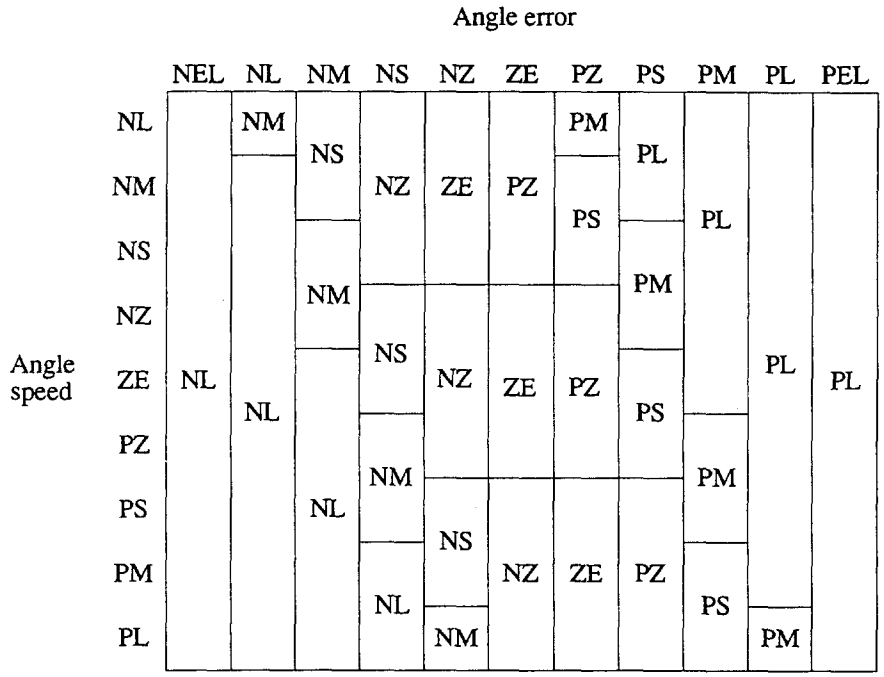

Fig. 13 Fuzzy relation matrix for control of arm angle or boom angle

The inference of the fuzzy relations is done in the fuzzy inference engine. It performs a fuzzy reasoning by using the fuzzy relations defined in the rule base and the definitions of the fuzzy sets found in the data base. With the premises, x is A' and y is B', it performs the fuzzy AND with the two antecedents of the fuzzy relation and then it uses the fuzzy relation function in order to calculate the consequent.

Let A and B be two fuzzy sets in U and V respectively, with membership functions $\mu_A(u)$ and $\mu_B(v)$ respectively. The AND operation then corresponds to the intersection $A \cap B$, where the result is characterized by its membership function $\mu_{A\cap B}(u, v)$. In this case, with the premises stated above, the result of the intersection becomes,

$$\mu_{A\cap B}(u_0, v_0) = \min\{\mu_A(u_0), \mu_B(v_0)\} \tag{21}$$

The fuzzy relation function used here is Mamdani's minimum operation rule. The result is a fuzzy set $C' = \{(w, \mu_{C'}(w)) \mid w \in W\}$ where the membership function is:

$$\mu_{C'}(w) = \mu_{A\cap B}(u_0, v_0) \cdot \mu_C(w) \tag{22}$$

Fig. 14 show the membership functions of the fuzzy sets for control of the arm cylinder, which are exactly the same for control of the boom cylinder.

The fuzzy set C' is deduced from the fuzzy relation IF x is A AND y is B THEN z is C with the premises x is A' and y is B'. However, the controller consist of a set of fuzzy relations, where the deduced fuzzy set from each fuzzy relation are connected using the fuzzy OR operation.

The OR operation between the two fuzzy sets A and B defined on the same universe of discourse W corresponds to the union $A \cup B$, where the union is characterized by its membership

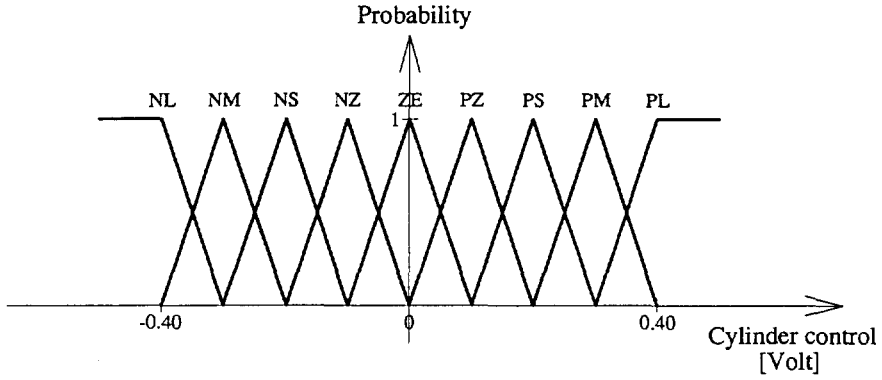

Fig. 14 Membership functions of the fuzzy sets defining fuzzy control value

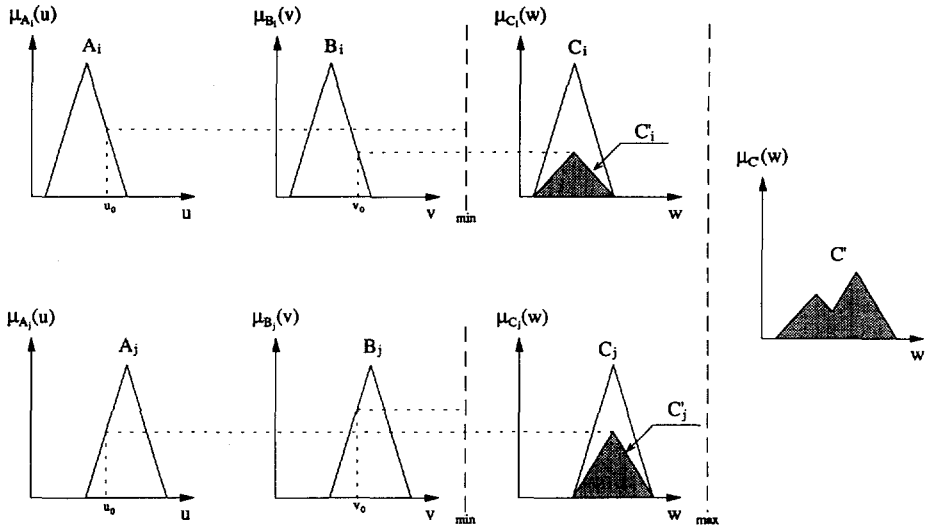

Fig. 15 Fuzzy inference

function $\mu_{AUB}(w)$ defined as,

$$\mu_{AUB}(w)=\max\{\mu_A(w), \mu_B(w)\} \tag{23}$$

The deduction of the control action according to (21), (22) and (23) is shown graphically in fig. 15.

When the fuzzy inference engine has made its decision on the fuzzy control action, the fuzzy value is converted into a crisp value by the defuzzyfier. The conversion is made using the center of area method (COA) which gives a smoothly varying output (LARKIN, 1985; SCHARF, 1985).Observe that the membership function of the fuzzy control value is discrete or quantized as shown in table 3 appendix J, which gives the defuzzyfication equation as,

$$c = \frac{\sum_{i=1}^{n} w_i \cdot \mu_c(w_i)}{\sum_{i=1}^{n} w_i} \tag{24}$$

where n is the number of quantization levels and w_i is defined in appendix J. Hence, the crisp control value, c, is real and can take any value in the same range as w. However, in order to increase the tuning ability a field tuning factor, k, is multiplied with the control value, c, and in order to further increase the stability of the controlled system the new control value, $k \cdot c$, is quantized to the same extent as for the generic elements of the fuzzy control value. But, the domain is increased to [−1.5 V, 1.5 V], since the hydraulic cylinders are working in the range [−3.2 V, −1.7 V] for contraction and [1.7 V, 3.2 V] for extension.

4 Experiments and Results

The experiments aimed at showing the FLC's ability to move the crane tip to a desired position and/or in a desired direction, and the controllers robustness. Some step responses of the boom and arm angle positioning are shown. A table showing the behavior of the straight line motion control is presented, and some sample plots of straight line movements are also shown, both with and without a load in the crane tip.

4.1 Tuning the FLC

There are a number of parameters to adjust in order to tune the FLC. Quantization levels, number of fuzzy sets and range of their support sets, and rules are the most obvious tuning parameters. These have already been set according to section 3.3, so here is the field tuning factor to be considered. In order to avoid overshoot, and a relatively smooth controller output, a value of 2.6 was chosen for the field tuning factor of the arm and boom angle controllers. In the step response experiments only one of the cylinders was controlled at a time. First a certain arm or boom angle was set, then the experiment started by giving a fixed angle reference to the arm or boom angle controller. Fig. 16a-b show some different, small and large, step responses for the arm and boom angles and the corresponding control signals are shown in fig. 16c-d.

A sine wave tracking experiment was also made in order to further investigate the controller stability and control output smoothness. Only one of the cylinders was controlled at a time. A sine wave was fed into each controller as a reference, representing the angle at different times. The frequency and amplitude was chosen in order to keep the required hydraulic flow less then the maximum hydraulic flow. In this case it also means that the controller output should seldom be at maximum ±1 Volt. Fig. 17a-d show the arm and boom angles and the controller outputs.

The sine wave tracking experiment showed that the arm and boom angles could follow the reference angle with a small time lag of about 200 ms. The time lag probably depends on dead time in the amplifiers and the electro−proportional valves. Notice that it does not seem to affect the robustness of the controlled system. The controller output for the arm cylinder seems to be a little more "nervous" than the output to the boom cylinder. It suggests that the field tuning factor could be somewhat reduced for the arm cylinder controller.

4.2 Straight line motion

After tuning the two controllers for each cylinder, some experiments were made transferring the crane tip along straight lines and investigating the speed of the straight line following. Now,

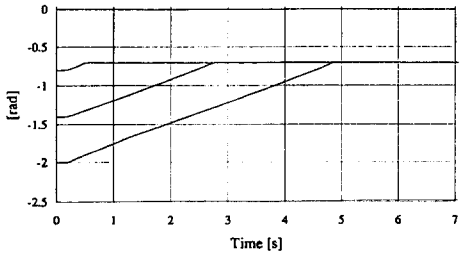

Fig. 16a Arm angle step responses

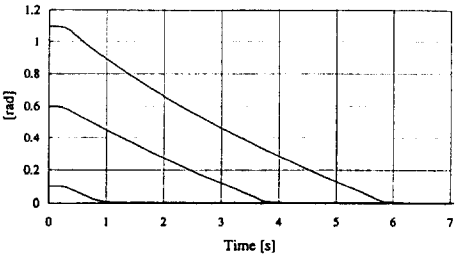

Fig. 16b Boom angle step responses

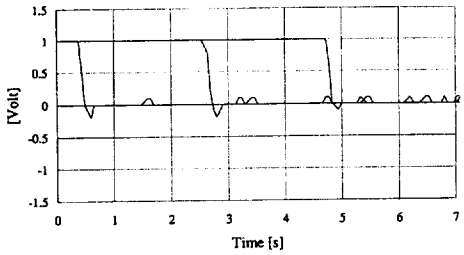

Fig. 16c Arm cylinder control voltages

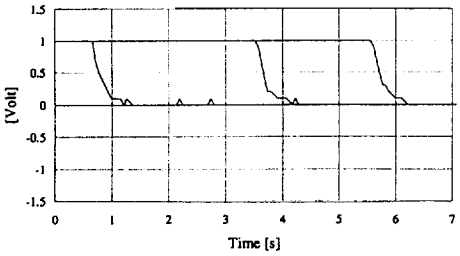

Fig. 16d Boom cylinder control voltages

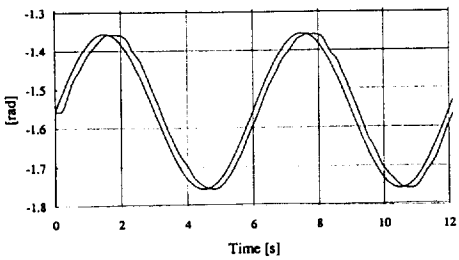

Fig. 17a Arm angle sine wave tracking

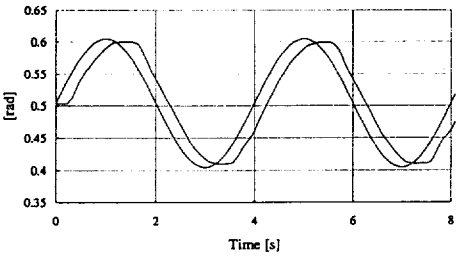

Fig. 17b Boom angle sine wave tracking

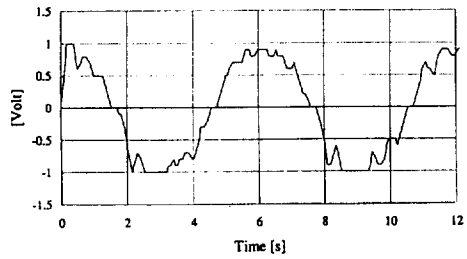

Fig. 17c Arm cylinder control voltage

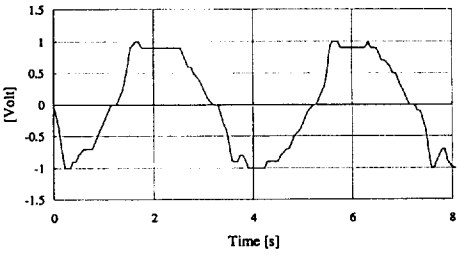

Fig. 17d Boom cylinder control voltage

both cylinders were operating at the same time, which caused some instability in the form of small oscillations of the arm and boom. In order to get a more stable behavior, the field tuning factors were changed to 2.2 for both the arm cylinder and boom cylinder controllers. This means that the maximum output was ± 0.8 Volt to both the arm and boom cylinders, which correspond to the maximum flow of approximately $P_{\alpha max}=10\ \ell$ /min for the boom cylinder and $P_{\alpha max}=13.5\ \ell$ / min for the arm cylinder.

Fig 18a-d show four experiments transferring the crane tip in a straight line. The maximum orthogonal distance error of the crane tip from the straight line between the starting point and the target point is 28 mm. The target positioning error is maximum 10 mm. Observe that this is the controller error, there is also an error in the sensors. In order to get a feeling for how large the total error distance from the straight line is, a straight rod was placed on the line that the crane tip was supposed to follow. The crane tip motion was then observed according to the straight rod. Without doing any measurements it could be seen that the crane tip stayed within ±5 cm from the reference line.

While the crane tip is moving along the straight line, the maximum possible crane tip speed is calculated at every sample period as described in section 3.2. The speed is multiplied with a constant, and the result is used for calculating the new reference position as input to the FLC. Through experiments it was found that the constant should be 0.75 which guarantees that the actual crane tip speed does not exceed the maximum possible crane tip speed. Fig. 19a-b show the crane tip speed and reference corresponding to fig. 18a and 18d respectively.

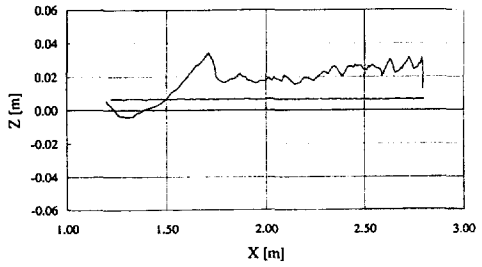

Fig. 18a Crane tip position and reference when moving from (1.196, 0.005) to (2.798, 0.007)

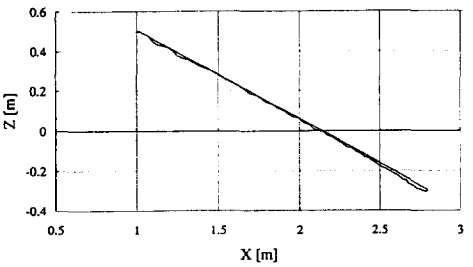

Fig. 18b Crane tip position and reference when moving from (2.797, −0.296) to (1.000, 0.500)

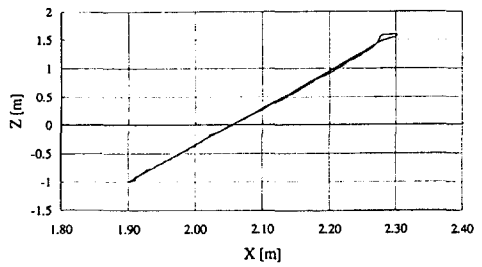

Fig. 18c Crane tip position and reference when moving from (1.899, −0.994) to (2.301, 1.600)

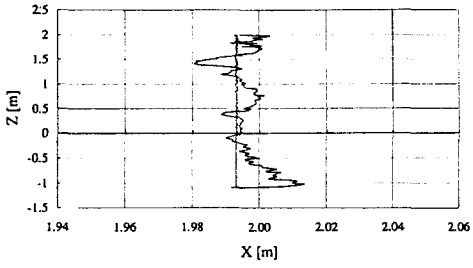

Fig. 18d Crane tip position and reference when moving from (1.996, 2.000) to (1.993, −1.096)

In order to investigate the robustness of the FLC, a weight of 440 kg was placed hanging from the crane tip. This weight was chosen because it was available, and a heavier one would have turned over the base machine. A tree in a final felling in Sweden typically weighs 300 to 500 kg. Fig. 20a-b show the motion of the crane tip in a straight line along the X-axis without and with the 440 kg weight. There is no substantial change in distance error, but the crane show a somewhat oscillating behavior in the position with the weight in the crane tip, however the amplitude of the oscillation is very small.

The oscillating behavior in fig. 20a and 20b is somewhat explained when looking at the arm and boom angle error and angular speeds which are the inputs to the controller, and when looking at the output voltages from the FLC. As can be seen in fig. 21a-f the FLC could be further tuned. A lower value of the field tuning factors could maybe make the behavior of the system more robust but it is not certainly so. The oscillation could also be the effect of the time delays in the proportional valves. Note however in fig. 21b and 21d, that the oscillation is somewhat larger in amplitude compared to fig. 21a and 21c with the 440 kg weight in the crane tip, especially for the boom cylinder.

4.3 Crane tip motion speed

Since the crane tip seemed to be able to follow a straight line with acceptable error, an investigation was made on how much slower this system is compared to a control system with no constraints on the used path. No constraints on the used path means that the crane tip should reach the target by setting the correct arm and boom angles as fast as possible, with no concern taken to the available amount of hydraulic fluid. Hence, the reference angles to the arm and boom cyl-

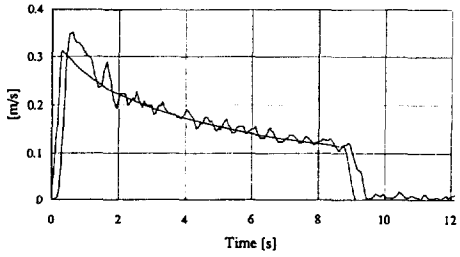

Fig. 19a Crane tip speed when moving from (1.196, 0.005) to (2.798, 0.007)

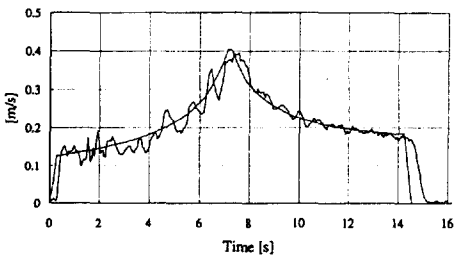

Fig. 19b Crane tip speed when moving from (1.996, 2.000) to (1.993, −1.096)

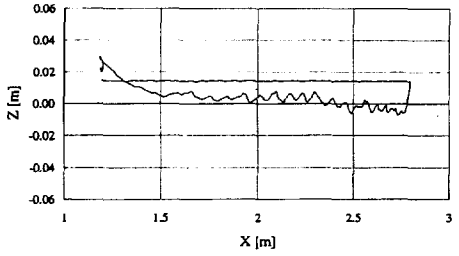

Fig. 20a Crane tip position and reference when moving from (2.795, 0.011) to (1.195, 0.015) with no load

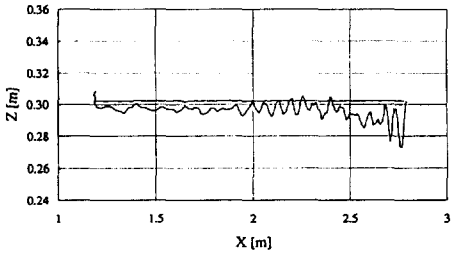

Fig. 20b Crane tip position and reference when moving from (2.789, 0.300) to (1.189, 0.302) with 440kg

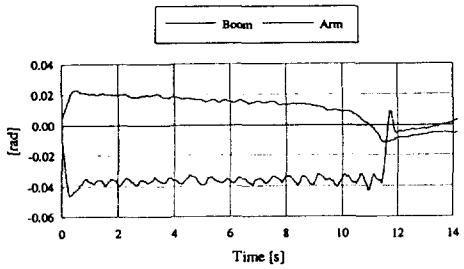

Fig. 21a Arm and boom cylinder error angles when moving from (2.795, 0.011) to (1.195, 0.015) with no load

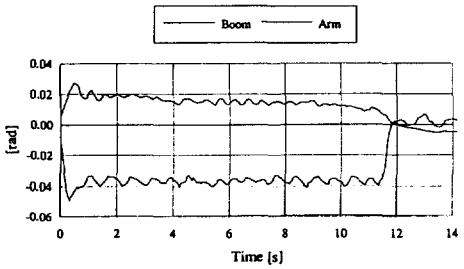

Fig. 21b Arm and boom cylinder error angles when moving from (2.789, 0.300) to (1.189, 0.302) with 440kg

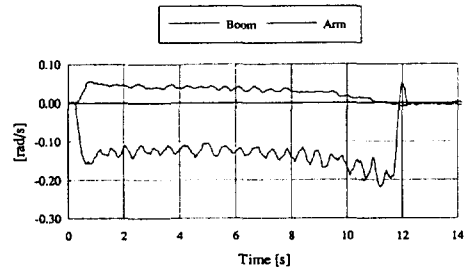

Fig. 21c Arm and boom cylinder angular speeds when moving from (2.795, 0.011) to (1.195, 0.015) with no load

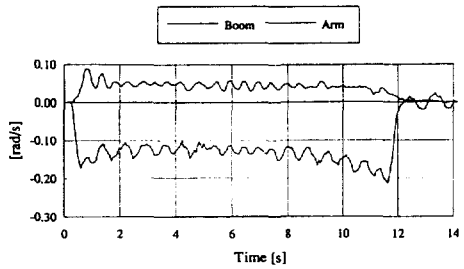

Fig. 21d Arm and boom cylinder angular speeds when moving from (2.789, 0.300) to (1.189, 0.302) with 440kg

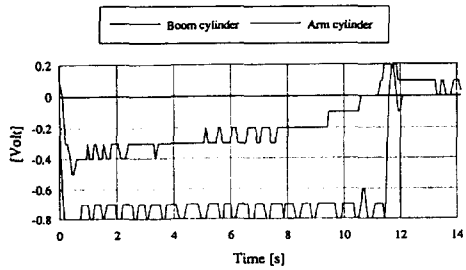

Fig. 21e Arm and boom cylinder control values when moving from (2.795, 0.011) to (1.195, 0.015) with no load

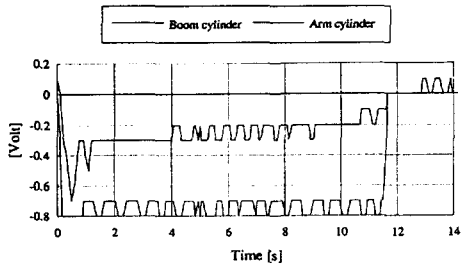

Fig. 21f Arm and boom cylinder control values when moving from (2.789, 0.300) to (1.189, 0.302) with 440kg

Table 2. Positioning time for different control strategies

Positioning	Fast	Straight
1	8.4 s	9.3 s
2	10.4 s	12.5 s
3	8.0 s	8.6 s
4	7.9 s	13.2 s
5	9.6 s	12.2 s

inder controllers of the "fast" system are the angles at which the crane tip is at the target position, while the reference angles to the controllers of the "straight" system are calculated so the crane tip will follow a straight line from the starting point to the target point. The FLC's in the two different systems were exactly the same. It was only the reference angles to the controllers that differed. Five different positionings were made with the two different reference input strategies. In both cases the positioning was halted when the boom tip was within 2 cm from the target position and the time used is shown in table 2.

On average, for the five positionings, it takes 27% longer time to move the crane tip along a straight path from the starting point to the target point, then just setting the correct angles of the arm and boom as fast as possible. However, the additional percentage of time used for the straight movement differ a lot with the start and target position. In positioning 4 (67%), the change of arm and boom angles are sequential, in order to move the crane tip along the straight line. While the boom angle is changing, the arm angle is hardly changed at all. Close to the target however, the arm angle is changed a lot while the boom angle is almost still. In positioning 3 (8%), the arm angle was changed very little, while the boom angle made all the work, in order to achieve a straight motion of the crane tip.

5 Discussion

The FLC is controlling the crane tip with an accuracy which is acceptable for the use in a forestry machine. This fundamental controller also seems to be very robust and was not affected by the 440 kg weight in the crane tip. The nonlinearities due to the mounting of the hydraulic cylinders, the non symmetric hydraulic cylinders, the constant change of load on the cylinders, and time lag in the proportional valves, are not affecting the robustness of the controlled system. However, oscillations with a small amplitude were found in the control values and cylinder extension/contraction speeds. It should be further investigated whether they depend on the time lag in the proportional valves, or maybe the quantization levels of the measured and controlled variables. It should be mentioned that the oscillations could only be detected in the measurements, and not by only watching the crane.

In some of the experiments it can be seen that the orthogonal error distance from the reference line always seem to have the same sign, i.e. the crane tip stays on the same side of the reference line from the starting point to the target. This implies that some kind of integration of this error should be performed and fed back to the controller. An other method could be to try the more aggressive defuzzyfication method mean of maxima (MOM).

Calculation of maximum possible crane tip speed also seems to work quite well. By always knowing the available amount of hydraulic fluid and keeping the required consumption at a lower level, no sudden "dips" in crane tip position will occur. However, the available amount of hydraulic fluid is determined by the size and rotational speed of the pump, and by the largest possible control value. In this case the output is restricted to ± 0.8 Volt by the value of the field tuning factor. A larger field tuning factor causes the cylinder control to become unstable even though the proportional valves are not fully open until the control value reaches ± 1.5 Volt. By having a wider support for the fuzzy sets close to the domain limits and more narrow support for the sets close to zero, it could be a solution to using the whole output range without stability problems.

Due to shortage of time an accurate measurement was not made of the crane tip position according to the reference line it was supposed to follow. One simple way of doing this is by using two potentiometers with a known distance from each other located in the plane of the crane, e.g. on the ground, and connected with wires to the crane tip. By triangulation, the correct path traveled by the crane tip can be calculated.

A natural extension of this project is of course to involve the rotation of the crane and the extender. By introducing these two actuators the crane tip can be controlled in three dimensions using four degrees of freedom. The extra degree of freedom could be used in order to minimize the use of hydraulic fluid, which will maximize the crane tip speed.

6 Preface

This project was driven during 8 months at Forestry and Forest Products Research Institute (FFPRI), In Tsukuba, Japan. It was sponsored by the Science and Technology Agency (STA) who financed one salary and FFPRI who stood for the squipment. We would like to thank the colleagues who somehow have been involved in this project and especially the colleagues at Automatic Control Laboratory, Mr. Mozuna and Mr. Yamaguchi.

7 References

BOVERIE, S., DEMAYA, B. and TITLI, A.: Fuzzy logic control compared with other automatic control approaches, IEEE Conference on decision and Control, 1 212-1 216 (1991)

BRAAE, M. and RUTHERFORD, D. A.: Fuzzy relations in a control setting, Kybernetes, **7** (3), 185-188 (1978)

DOTE, Y.: Stability analysis of variable structured controller by fuzzy logic for servo system, IEEE Conference on decision and control, **2**, 1 217-1 218 (1991)

GRAHAM, B. P. and NEWELL, R. B.: Fuzzy adaptive control of a first order process, Fuzzy sets and systems, (31), 47-65 (1989)

KING, P. J. and MAMDANI, E. H. : Application of Fuzzy Control systems to industrial processes, Automatica, **13**, 235-242 (1977)

KOSKINEN, H.: Fuzzy control strategies for active magnetic bearings, Fuzziness, 12 pp. (1993)

LARKIN, L. I.: A fuzzy logic controller for aircraft flight control, Industrial Applications of Fuzzy Control, 87-103 (1985)

LEE, C. C.: Fuzzy logic in control systems: Fuzzy logic controller—Part I, IEEE Transactions on systems, man, and cybernetics, **20** (2), 404-418 (1990 a)

———: Fuzzy logic in control systems: Fuzzy logic controller-Part II, IEEE Transactions on

systems, man, and cybernetics, **20** (2), 419-435 (1990 b)

LÖFGREN, B.: Crane tip control, Meddelande, Forskningsstiftelsen Skogsarbeten, (18), 77pp. (1989)

MOZUNA, M., ASAHI, K. and FUKUDA, A.: The motion control of a feller buncher's head (II)-Design of the man-machine interface, Transactions of the 3rd annual meeting of Japanese Forestry Society, 685-686 (1992)

PROCYK, T. J. and MAMDANI, E. H.: A linguistic self−organizing process controller, Automatica, (15), 15-30 (1979)

SCHARF, E. M. and MANDIC, N. J.: The application of a fuzzy controller to the control of a multi-degree-freedom robot arm, Industrial Applications of Fuzzy Control, 41-62 (1985)

SMITH, S. M. and COMER, D. J.: Automated calibration of a fuzzy logic controller using a cell state space algorithm, IEEE Control system magazine, **11** (5), 18-28 (1991)

SRIPADA, N. R., FISHER, D. G. and MORRIS, A. J.: AI application for process regulation and servo control, IEEE Proceedings, **134** (4), 251-259 (1987)

UCHINO, T., NARISAWA, J., SATO, Y. and KUMAZAWA, K.: Multi-jointed pile driving machine with a computer-assisted guiding system, Automation and Robotics in Construction X, 363-370 (1993)

VIRVALO, T. and KOSKINEN, H.: Fuzzy logic controller for hydraulic drives, Aachener fluidtechnisches kolloquium, 225-240 (1992)

YASUNOBU, S., MIYAMOTO, T. and IHARA, H.: Fuzzy control for automatic train operation system, IFAC Control in transportation systems, 33-39 (1983)

——— and MIYAMOTO, T.: Evaluation of an automatic container crane operation system based on predictive fuzzy control, Control theory and advanced technology, **2** (3), 419-432 (1986).

——— and HASEGAWA, S.: Automatic train operation system by predictive fuzzy control, Industrial applications of fuzzy control, 18 pp. (1985)

ZADEH, L. A.: Outline of a new approach to the analysis of complex systems and decision processes, IEEE Transactions on systems, man, and cybernetics, **3** (1), 28-44 (1973)

林業機械用ナックルブームクレーンのファジィ制御

ASPLUND, Christer (1)　福田章史(2)

摘　要

本論文は林業機械のナックルブームクレーンの制御システムについて研究を行ったものである。現在北欧諸国，北米などで用いられている多くの林業機械は，クレーンで材の積み込み積み下ろしを行い，またハーベスタヘッドやプロセッサヘッドなどの作業機を車両に搭載したクレーンの先端に取り付け，高能率の作業を行っている。これらのクレーンの形式はほとんどがナックルブーム式である。日本においてもこれらの機械が近年多く使用されはじめており，生産性の向上，安全な作業，林地を荒らさない作業を目指して地形条件や作業方法などの日本の環境に適合した機械の開発が進められている。しかし，ナックルブームクレーンは多数の油圧シリンダ，油圧モータにより動かされているが，現在のところ，この運転はこれらに直接接続された多数のレバーを同時操作することで行っており，運転手の負担も多く，運転には習熟が必要である。

本研究の目的は，ジョイスティックなどを用いた簡単な操作で，クレーンの先端を指示した目標位置へ指示した経路で移動させる制御システムを開発することである。またこの制御システムは，クレーンの先端を現在位置から目的位置へ設定した経路に沿ってできるだけ速く移動させることを目的としている。この経路は必ずしも直線ではなく，任意の経路を設定することができる。

目標位置は運転手がその位置をジョイスティックで直接指示したり，高度なセンサによって立木の位置を自動的に識別しこれを目標位置としたり，あるいは途中の障害物を検知して適切な経路を設定したりすることが考えられるが，本研究では，目標位置はこれらの方法で与えられたものとしてアームとブームの油圧シリンダを制御する方法について検討した。

クレーンの先端を目標位置へ移動させるには，これらの油圧シリンダを協調して制御しなければならない。また，クレーン先端の移動速度は，油圧ポンプの吐出容量や回転速度に規制され，さらにクレーンの位置によって必要な油圧流量が変化する。従って，目標位置が外部から与えられたとしても，機械の運転には高度な制御が必要となる。

このシステムの制御にはファジィ論理制御(Fuzzy Logic Controler, FLC)を用いた。本論文ではFLCの基礎となるファジィ集合及び今回設計したFLCの基礎的な特性について述べている。さらに，森林総合研究所で試作した車両に本研究で開発したファジィ制御プログラムを載せて実験を行い，プログラムの評価を行った結果について述べている。さらに，森林総合研究所で試作した車両に本研究で開発したファジィ制御システムを載せて実験を行い，プログラムの評価を行った結果について述べている。

1994年2月2日受理

(1)　スウェーデン農科大学林学部（1993年4月から11月まで，
STAフェローシップの客員研究員として生産技術部に在籍）
(2)　生産技術部

試験に使用した機械は，Fig. 1, 2に示したもので，ナックルブームはブーム，アーム，エクステンションブーム，旋回装置から構成され，これらは油圧シリンダあるいは油圧モータで駆動している。そしてこれらの油圧アクチュエータは，電磁流量制御バルブで制御されるが，これに与える信号をコンピュータからD／Aコンバータを介して出力した。使用したセンサはブームとアームの角度を検出するポテンショメータである。制御プログラムは全てC言語で作成した。

今回の試験は，ブームとアームの角度のみを制御した。ブームとアームの幾何学的構造はFig. 3に示した。クレーン先端が移動可能な範囲をFig. 4に示した。おのおのの角度とシリンダの伸縮量の関係は，Fig. 5に示した。クレーン先端の座標とブーム，アーム角の関係を表す運動学方程式は式(1)，(2)に，その逆関数は式(3)，(4)に示した。またこれらの速度を求める式を式(5)から(12)に示した。シリンダの伸縮量とブーム，アーム角の関係を式(13)，(14)に，ブーム，アームシリンダの速度とブーム，アームの角速度の関係を式(15)，(16)に示した。

本論文での制御システムの考え方は，目的位置までできるだけ速く，そして現在位置と目標位置を結んだ経路上をクレーン先端が誤差なく移動するようにすることである。制御システムの全体の構成はFig. 6のブロック図に示した。ここでは目標値の座標を運動学方程式の逆関数からブーム，アーム角に換算し，この値とセンサで測定したそれぞれの角度の差を誤差量として制御装置に入力している。

この目標値は，現在位置と目標位置を結んだ経路上に70 msecの制御サイクルごとに設定される。用いている油圧回路の最大流量の制限から，現実の機械はシリンダの速度に制限があり，しかもこの制限はクレーン先端の位置により常に変動する。従って運転手の指示した速度を下回った速度で動かさなければならない事態も生じ，その時には目標値も変化する。この点について3. 2節で詳しく論じた。

FLCは，コンピュータのプログラムで実現したが，その構成をFig. 10に示している。ファジィ化のための入力データの量子化についてはTable 1及びAppendix　Jに示した。入力値のメンバーシップ関数をFig. 11，12に示した。また，用いたファジィルールをFig. 13に，非ファジィ化のための出力のメンバーシップ関数をFig. 14に示した。

出力についても，油圧回路の流量の制限からその値をそのまま流量制御バルブに送ることはできない。そこでこの出力に係数を乗じて実際の出力値とした。この係数は現場チューニング係数と呼び現場試験で求めたが，これについての詳しい説明を4. 1節で述べている。

ステップ応答試験，サインカーブによる追随試験を行い現場チューニング係数を決定した。

また，440 kgの荷重をクレーンの先端につるした負荷状態と，無負荷状態での直線移動の試験を行い，システムの変動に対する強さ（ロバスト性）を調べた。さらにクレーン先端の移動速度について，移動経路が直線上を追随しないが速度が速い場合と，速度は遅くなるが直線上を追随させた場合の比較を行なった（Table 2）。

試験の結果，現場チューニング係数を2. 2ないし2. 6とすることで，オーバーシュートの少ない安定した制御が行えた（Fig. 16，17）。また，ファジィ制御プログラムは油圧回路及びクレーンの設計からくる非線形性にもかかわらずロバスト性の高い結果を示した。クレーンの先端に作業機を想定して440 kgの重量をつるした場合でも，やはりロバスト性の高い結果を示した（Fig. 18～21）。クレーン先端が初

期位置と目標位置を直線で結んだ線上を移動するように制御した結果，クレーン先端の軌跡の垂直方向の誤差は3cm以下であり，センサの誤差を含んでも5cm以下であった。これらの誤差はこのナックルブームクレーンを林業作業用に用いるためには十分小さいものと考えられる。このシステムの場合，制御を安定させるために流量制御バルブへの出力をその最大値である±1.5Vを±0.8Vの範囲に現場チューニング係数で制限する必要があった。初期位置から目標位置までの直線上を誤差なく移動させたときの移動時間は，直線からの誤差を考慮しないで移動させた場合に比べ約30%の遅れが見られた。これらはこのシステムの問題点であるが，本論文ではこの点についていくつかの解決方法を提案している（5章）。

結論的にいえばFLCは従来の制御方法に比較してより有利な制御方法であり，クレーンのコントロールシステムとして有効な手段であるといえよう。今後，この制御にクレーンの回転とエクステンションブームの制御を加えて3次元での制御に発展させていくことが考えられる。

Appendix A The hydraulic system

The hydraulic system consist of a hydraulic pump powered by the diesel engine and four actuators : a rotational motor and three cylinders. Fig. 1 show a schedule of the system.

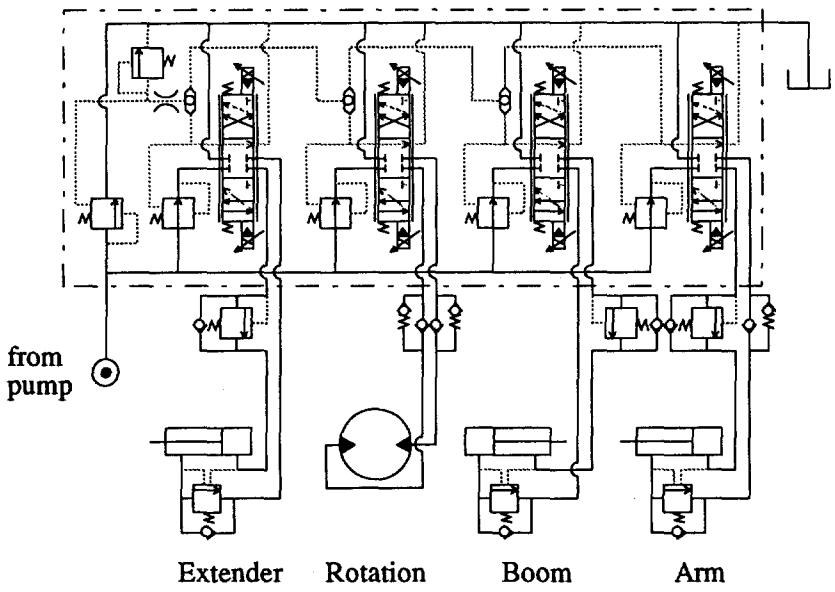

Fig. 1 Schedule of the knuckle boom crane hydraulic system

In table 1 data on the pump and the actuators can be found. The hydraulic pump is directly powered by the diesel engine, which has a maximum rotational speed of 2800 rev/min. Between the hydraulic rotational motor and the crane pillar is a gear with ratio 6.5 : 1.

Table 1. Data for hydraulic pump and actuators.

Hydraulic pump	Type	Nachi IPH-4A-20-12
	Displacement	20.7 cm^3/rev
	Maximum pressure	175 MPa (adjustable)
	Efficiency	0.94
Rotational motor	Type	Nachi PC-100-19-1B-0864
	Displacement	20.7 cm^3/rev
	Maximum torque	552 Nm
	Maximum flow	22 ℓ /min
Boom cylinder	Type	Kobayashi
	Min length	517 mm
	Max length	802 mm
	Piston diameter	90 mm
	Piston rod diameter	45 mm
	Max flow	23 ± 3 ℓ /min
	Max pressure	17.2 MPa
Arm cylinder	Type	Kobayashi
	Min length	582 mm
	Max length	932 mm
	Piston diameter	90 mm
	Piston rod diameter	40 mm
	Max flow	23 ± 3 ℓ /min
	Max pressure	17.2 MPa
Extension cylinder	Type	Kobayashi
	Min length	862 mm
	Max length	1 232 mm
	Piston diameter	80 mm
	Piston rod diameter	40 mm
	Max flow	45 ± 5 ℓ /min
	Max pressure	17.2 MPa

Appendix B Angle accuracy using potentiometer sensors

The angle between the crane pillar and the boom, β, and the angle between the boom and the arm, α, are measured using angular potentiometers CP-2UP (β) and CP-3UY (α) manufactured by Midori Precisions Co. The 0-5 volt potentiometer signal is converted to a digital signal using a 12 bit A/D converter. The resolution of the angular sensors are given in table 1.

Howerver, due to electrical noise, the sensor signals are fluctuating. α was measured when the crane structure was not moving and 100 observation are shown in fig. 1. The mean value is at 1 349, and the standard deviation is 2.1 (bits), with a maximum error of 5 bits. In order to improve the measurement of the angle, a number of measurements, n, can be made. The calculated average can then represent the angle at the current sample time. This requires that the total time for the n A/D conversions is short in comparison with the sample time. Two measurements consisting of 100 observations each, with different values on n are shown in fig. 2 and 3. Corresponding mean values and standard deviations are shown in table 2.

Table 1. Theoretical resolution of angular sensors

	[bits/rad]	[rad/bit]
Arm angle, α	1 801	$5.55 \cdot 10^{-4}$
Boom angle, β	2 409	$4.15 \cdot 10^{-4}$

Table 2. Statistical data for different arm angle measurement methods

n	mean	std	min	max
1	1 349	2.1	−5	+5
5	1 352	1.0	−2	+2
30	1 355	0.7	−2	+2

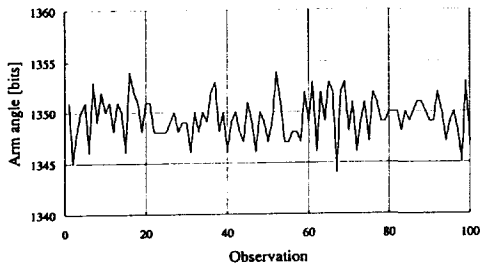

Fig. 1　$n=1$ measurement per observation point

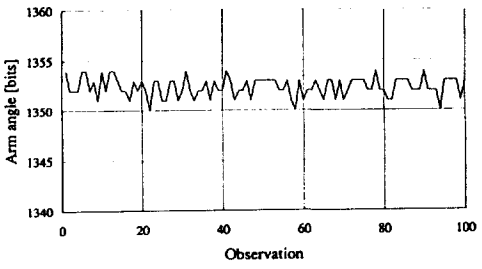

Fig. 2　$n=5$ measurements per observation point

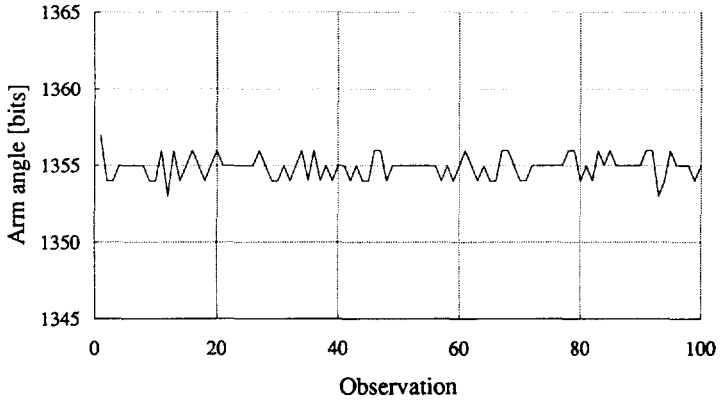

Fig. 3 $n=30$ measurements per observation point

Appendix C Angular speed accuracy and filtering

The angular speed between the crane pillar and the boom, $d\beta/dt$, and the angular speed between the boom and the arm, $d\alpha/dt$, are calculated from the angle measurements as mentioned in section 3.3. A simple approach to calculate the speed is to take the change in bits over one sample and divide with the sample time. In fig. 1 the result from such a calculation is shown when the arm angle is measured with a sample time of 70 ms. As can be seen the signal is quite noisy, due to electrical noise, and to vibrations in the mechanical structure of the crane and the mounting of the potentiometer. There is also noise produced by the calculation since the sample time in this case can have an error of ± 10 ms. Since the sampling time is not constant, a digital filter is not easily constructed. But a simple filter would be to calculate some kind of moving average. In this application the speed is calculated according to,

$$\frac{d\alpha}{dt} = \frac{\alpha(k)-\alpha(k-d)}{t(k)-t(k-d)} \tag{1}$$

where, k is the current sample

d is number of samples to look in the past

$\alpha(k)$ is the arm angle at sample k

$t(k)$ is the time at sample k

In fig. 2, the calculated arm angular speed is shown, using the same data as used in fig. 1, when $d=2$, and in fig. 3 when $d=4$.

Fig. 4 shows the angular speed when the angle measurement has been improved, using the method described in appendix B, with $n=30$. The speed is then calculated with $d=4$. The same data is not used as in fig. 3. There is no obvious difference in the smoothness of the speed signal between fig. 3 and 4.

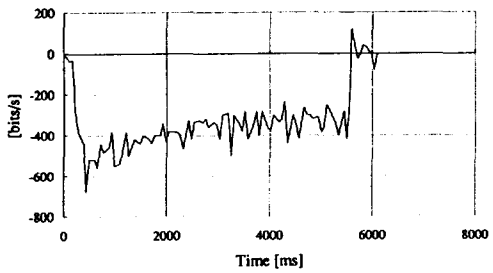

Fig. 1　Speed calculated with $d=1$

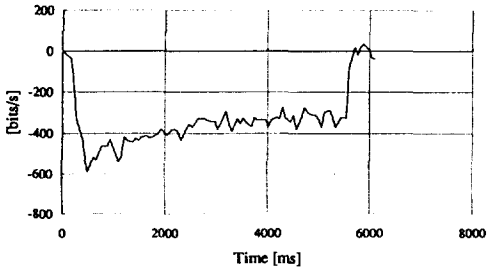

Fig. 2　Speed calculated with $d=2$

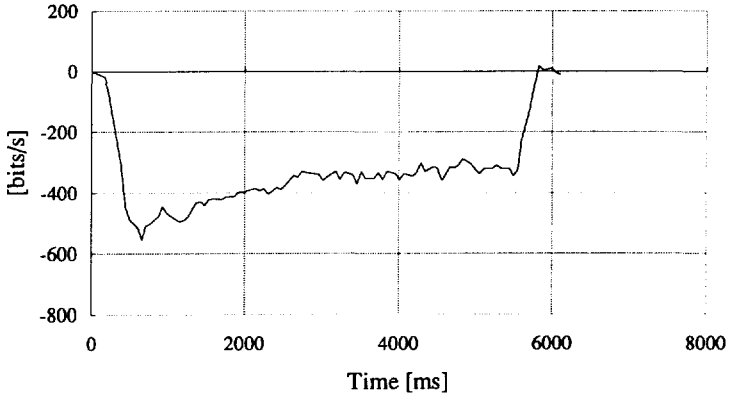

Fig. 3 Speed calculated with $d=4$

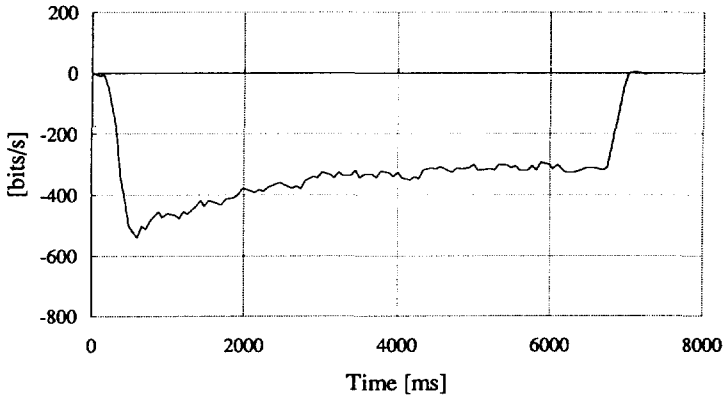

Fig. 4 Speed calculated with $d=4$ and $n=30$

Appendix D Crane kinematics and it's inverse

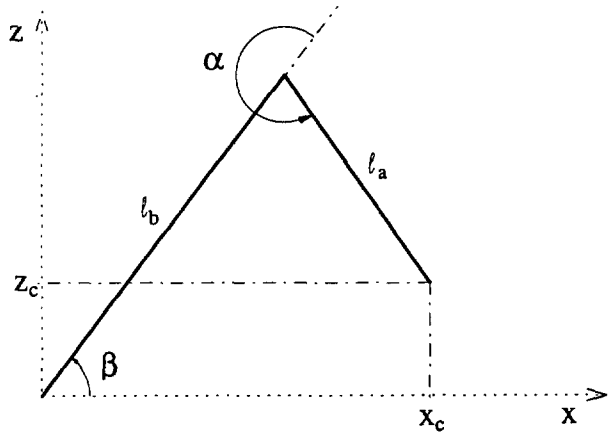

Fig. 1 Schematic drawing of the knuckle boom crane

1) Kinematics, i.e. calculation of the coordinates in the orthogonal coordinate system from arm angle, $\alpha(t)$, and boom angle, $\beta(t)$.
It can easily be seen that,

$$x_c(t) = l_b \cos\beta(t) + l_a \cos(\alpha(t) + \beta(t)) \tag{1}$$

$$z_c(t) = l_b \sin\beta(t) + l_a \sin(\alpha(t) + \beta(t)) \tag{2}$$

2) Inverse kinematics, i.e. calculation of $\alpha(t)$ and $\beta(t)$ when the crane tip coordinate is known.

The cosine theorem and Pythagoras theorem gives,

$$x_c(t)^2 + z_c(t)^2 = l_a^2 + l_b^2 - 2\, l_a l_b \cos(\alpha(t) - \pi) \tag{3}$$

$$l_a^2 = x_c(t)^2 + z_c(t)^2 + l_b^2 - 2\, l_b \sqrt{x_c(t)^2 + z_c(t)^2} \cos\left[\beta(t) - \arctan\left(\frac{z_c(t)}{x_c(t)}\right)\right] \tag{4}$$

from (3) and (4) the angles can be calculated,

$$\alpha(t) = \arccos\left(\frac{x_c(t)^2 + z_c(t)^2 - l_a^2 - l_b^2}{-2\, l_a l_b}\right) + \pi \tag{5}$$

$$\beta(t) = \arccos\left(\frac{l_a^2 - l_b^2 - x_c(t)^2 - z_c(t)^2}{-2\, l_b \sqrt{x_c(t)^2 + z_c(t)^2}}\right) + \arctan\left(\frac{z_c(t)}{x_c(t)}\right) \tag{6}$$

Appendix E Crane tip speed

Calculations of the equations that describe the crane tip speed in the orthogonal coordinate system when the arm and boom angular velocities are known, are shown here. How the inverse equations are calculated is also described.

The crane tip position is calculated using the equations described in appendix D, repeated here,

$$x_c(t) = l_b\cos\beta(t) + l_a\cos(\alpha(t)+\beta(t)) \tag{1}$$

$$z_c(t) = l_b\sin\beta(t) + l_a\sin(\alpha(t)+\beta(t)) \tag{2}$$

where,

x_c=position in x coordinate
z_c=position in z coordinate
$\alpha(t)$=angle between arm and boom, called arm angle
$\beta(t)$=angle between crane pillar and boom, called boom angle

In order to get the speed, the time derivative is taken of (1) and (2),

$$\dot{x}_c(t) = g_1 \cdot \dot{\alpha}(t) + g_2 \cdot \dot{\beta}(t) \tag{3}$$

$$\dot{z}_c(t) = g_3 \cdot \dot{\alpha}(t) + g_4 \cdot \dot{\beta}(t) \tag{4}$$

where,

$$g_1 = g_1(\alpha(t),\ \beta(t)) = -l_a\sin(\alpha(t)+\beta(t)) \tag{5}$$

$$g_2 = g_2(\alpha(t),\ \beta(t)) = -l_b\sin\beta(t) - l_a\sin(\alpha(t)+\beta(t)) \tag{6}$$

$$g_3 = g_3(\alpha(t),\ \beta(t)) = l_a\cos(\alpha(t)+\beta(t)) \tag{7}$$

$$g_4 = g_4(\alpha(t),\ \beta(t)) = l_b\cos\beta(t) + l_a\cos(\alpha(t)+\beta(t)) \tag{8}$$

If the crane tip speed is known, the arm and boom angular velocities can be calculated by solving equations (5) and (6),

$$\dot{\alpha}(t) = \frac{g_4}{g_1g_4 - g_2g_3}\cdot\dot{x}_c(t) - \frac{g_2}{g_1g_4 - g_2g_3}\cdot\dot{z}_c(t) \tag{9}$$

$$\dot{\beta}(t) = \frac{g_3}{g_1g_4 - g_2g_3}\cdot\dot{x}_c(t) + \frac{g_1}{g_1g_4 - g_2g_3}\cdot\dot{z}_c(t) \tag{10}$$

Appendix F Arm and boom cylinder lengths

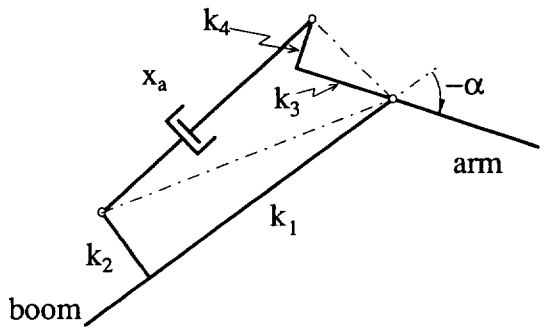

Fig. 1 Arm cylinder mounting between arm and boom

1) Arm cylinder length

From fig. 1 the cosines theorem gives,

$$x_a(t)^2 = k_1^2 + k_2^2 + k_3^2 + k_4^2 - 2\sqrt{k_1^2+k_2^2}\sqrt{k_3^2+k_4^2}\cos(\theta_1 - \alpha(t)) \tag{1}$$

where,

$k_1 = 0.743\ m$
$k_2 = 0.244\ m$
$k_3 = 0.210\ m$
$k_4 = 0.045\ m$

$$\theta_1 = \arctan\left(\frac{k_4}{k_3}\right) - \arctan\left(\frac{k_2}{k_1}\right) \approx -0.10621\ rad$$

hence, the arm cylinder length can be calculated using,

$$x_a(t) = \sqrt{c_1 + c_2\cos(\theta_1 - \alpha(t))} \tag{2}$$

where,

$c_1 = k_1^2 + k_2^2 + k_3^2 + k_4^2 = 0.65771\ m^2$

$c_2 = -2\sqrt{k_1^2+k_2^2}\sqrt{k_3^2+k_4^2} \approx -0.33591\ m^2$

2) Boom cylinder length

From fig. 2 the cosines theorem gives,

$$x_b(t)^2 = k_5^2 + k_6^2 + k_7^2 + k_8^2 - 2\sqrt{k_5^2+k_6^2}\sqrt{k_7^2+k_8^2}\cos(\theta_2 - \beta(t)) \tag{3}$$

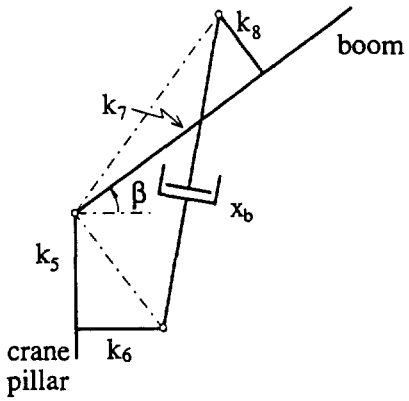

Fig. 2 Boom cylinder mounting between crane pillar and boom

where,

$k_5 = 0.247\ m$

$k_6 = 0.142\ m$

$k_7 = 0.544\ m$

$k_8 = 0.119\ m$

$$\theta_2 = \arctan\left(\frac{k_8}{k_7}\right) - \arctan\left(\frac{k_6}{k_5}\right) + \frac{\pi}{2} \approx 1.26440\ rad$$

hence, the boom cylinder length can be calculated using,

$$x_b(t) = \sqrt{c_3 + c_4\cos(\theta_2 - \beta(t))} \tag{4}$$

where,

$$c_3 = k_5^2 + k_6^2 + k_7^2 + k_8^2 = 0.39127\ m^2$$

$$c_4 = -2\sqrt{k_5^2+k_6^2}\sqrt{k_7^2+k_8^2} \approx -0.31731\ m^2$$

Appendix G Arm and boom cylinder speeds

The arm and boom cylinder lengths, x_a (t) and x_b (t), are calculated from the arm and boom angle respectively using the functions described in appendix F, which are repeated here,

$$x_a(t) = \sqrt{c_1 + c_2 \cos(\theta_1 - \alpha(t))} \tag{1}$$

$$x_b(t) = \sqrt{c_3 + c_4 \cos(\theta_2 - \beta(t))} \tag{2}$$

Where c_1, c_2, c_3, c_4 and θ_1, θ_2 are defined in appendix F.

The cylinder speeds are calculated taking the time derivative of (1) and (2),

$$\dot{x}_a(t) = g_5 \dot{\alpha}(t) \tag{3}$$

$$\dot{x}_b(t) = g_6 \dot{\beta}(t) \tag{4}$$

where,

$$g_5 = g_5(\alpha(t)) = \frac{c_2 \sin(\theta_1 - \alpha(t))}{2\sqrt{c_1 + c_2 \cos(\theta_1 - \alpha(t))}} \tag{5}$$

$$g_6 = g_6(\beta(t)) = -\frac{c_4 \sin(\theta_2 + \beta(t))}{2\sqrt{c_3 + c_4 \cos(\theta_2 - \beta(t))}} \tag{6}$$

If the cylinder speeds are known then the angular speeds can be calculated by solving (3) and (4),

$$\dot{\alpha}(t) = \frac{1}{g_5} \dot{x}_a(t) \tag{7}$$

$$\dot{\beta}(t) = \frac{1}{g_6} \dot{x}_b(t) \tag{8}$$

Appendix H Cylinder flow rates

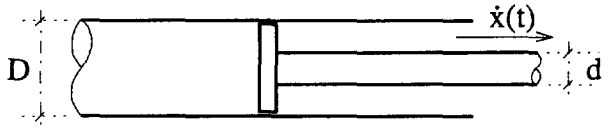

Fig. 1 Hydraulic cylinder

When the arm and boom cylinders are extending they will require more hydraulic fluid then when they are extracting due to the construction of the cylinders (fig. 1), i.e. the piston rod is only taking up volume on one side of the piston. The flowrate is defined as the change in volume per time unit. It is also defined to be positive when the cylinder is extending and negative when the cylinder is extracting. The hydraulic flow to the arm cylinder, $P_a(t)$, and boom cylinder, $P_b(t)$ are,

$$P_a(t) = g_7(\dot{x}_a(t)) \cdot \dot{x}_a(t) \tag{1}$$

$$P_b(t) = g_8(\dot{x}_b(t)) \cdot \dot{x}_b(t) \tag{2}$$

With the diameters for the arm and boom cylinders

$D_a = 0.090\ m$

$d_a = 0.040\ m$

$D_b = 0.090\ m$

$d_b = 0.045\ m$

g_7 and g_8 becomes,

$$g_7 = g_7(v) = \begin{cases} \dfrac{\pi D_a^2}{4} \approx 6.36173 \cdot 10^{-3}, & v \geqq 0 \\ \dfrac{\pi (D_a^2 - d_a^2)}{4} \approx 5.10509 \cdot 10^{-3}, & v < 0 \end{cases}$$

$$g_8 = g_8(v) = \begin{cases} \dfrac{\pi D_b^2}{4} \approx 6.36173 \cdot 10^{-3}, & v \geqq 0 \\ \dfrac{\pi (D_b^2 - d_b^2)}{4} \approx 4.77129 \cdot 10^{-3}, & v < 0 \end{cases}$$

When the hydraulic flow is known the cylinder extension speeds can be calculated,

$$\dot{x}_a(t) = \frac{1}{g_7(P_a(t))} \cdot P_a(t) \tag{3}$$

$$\dot{x}_b(t) = \frac{1}{g_8(P_b(t))} \cdot P_b(t) \tag{4}$$

Appendix I Maximum crane tip speed

Since the amount of hydraulic fluid is limited it will determine the crane tip maximum speed in a desired direction. It is of interest to know this speed since it is changing with the current arm and boom angles and in order to avoid too excessive reference values to the controllers.

The desired direction of motion of the crane tip can be written as,

$$c=\frac{\dot{z}_c(t)}{\dot{x}_c(t)} \tag{1}$$

The crane tip speed is a function of the arm and boom angular speeds which is according to appendix E,

$$\dot{x}_c(t)=g_1\cdot\dot{\alpha}(t)+g_2\cdot\dot{\beta}(t) \tag{2}$$

$$\dot{z}_c(t)=g_3\cdot\dot{\alpha}(t)+g_4\cdot\dot{\beta}(t) \tag{3}$$

and the arm and boom angular speeds are functions of each cylinders speed according to appendix G,

$$\dot{\alpha}(t)=\frac{1}{g_5}\ \dot{x}_a(t) \tag{4}$$

$$\dot{\beta}(t)=\frac{1}{g_6}\ \dot{x}_b(t) \tag{5}$$

and finally, the cylinder speeds are functions of the flow rates according to appendix H,

$$\dot{x}_a(t)=\frac{1}{g_7}\ P_a(t) \tag{6}$$

$$\dot{x}_b(t)=\frac{1}{g_8}\ P_b(t) \tag{7}$$

Hence, the desired direction of crane tip motion c, can be written as,

$$c=\frac{g_3g_6g_8P_a(t)+g_4g_5g_7P_b(t)}{g_1g_6g_8P_a(t)+g_2g_5g_7P_b(t)} \tag{8}$$

Since c is known, the relation between the flow to the arm and boom cylinder can be written as,

$$P_a(t) = \frac{1}{g} P_b(t) \tag{9}$$

where,

$$g = \begin{cases} -\dfrac{g_6 g_8 (g_3 - c g_1)}{g_5 g_7 (g_4 - c g_2)} & |c| < 1 \\ -\dfrac{g_6 g_8 (g_3/c - g_1)}{g_5 g_7 (g_4/c - g_2)} & |c| \geq 1 \end{cases} \tag{10}$$

In order to avoid numerical problems in a computer the factor g describing the relationship between the hydraulic flow to the arm and boom cylinders should be calculated according to equation (10). Notice also that the factors g_7 and g_8 are depending on the direction of motion of the arm and boom cylinders. When the calculation of g is made, the arm and boom angular speeds could be used as argument to g_7 and g_8 respectively. These speeds are calculated using (2) and(3). Observe that it is only the sign of the angular speeds that effects the result.

Since the available hydraulic flow is limited to P_{max} the flow to the arm cylinder, $P_a(t)$, and boom cylinder, $P_b(t)$, can be determined. However, the flow is defined to be positive when a cylinder is extending and negative when contracting. This means that the flow equality equation must be written as,

$$P_{max} = |P_a(t)| + |P_b(t)| \tag{11}$$

Equation (11) can be divided into four special cases where (9) is used.

1) $P_a(t) \geq 0$ and $P_b(t) \geq 0$ which gives,

$$P_{max} = P_a(t) + P_b(t) \tag{12}$$

(9) and (12) gives,

$$P_a(t) = \frac{1}{1+g} P_{max} \tag{13}$$

$$P_b(t) = -P_a(t) + P_{max} \tag{14}$$

2) $P_a(t) \geq 0$ and $P_b(t) < 0$ which gives,

$$P_{max} = P_a(t) - P_b(t) \tag{15}$$

(9) and (15) gives,

$$P_a(t)=\frac{1}{1-g}\ P_{\max} \tag{16}$$

$$P_b(t)=P_a(t)-P_{\max} \tag{17}$$

3) $P_a(t)<0$ and $P_b(t)\geqq 0$ which gives,

$$P_{\max}=-P_a(t)+P_b(t) \tag{18}$$

(9) and (18) gives,

$$P_a(t)=-\frac{1}{1-g}\ P_{\max} \tag{19}$$

$$P_b(t)=P_a(t)+P_{\max} \tag{20}$$

4) $P_a(t)<0$ and $P_b(t)<0$ which gives,

$$P_{\max}=-P_a(t)-P_b(t) \tag{21}$$

(9) and (21) gives,

$$P_a(t)=-\frac{1}{1+g}\ P_{\max} \tag{22}$$

$$P_b(t)=-P_a(t)-P_{\max} \tag{23}$$

Since $P_a(t)$ and $P_b(t)$ are known it is a simple task to calculate the maximum crane tip speeds from equation (2) to (7). Hence,

$$\dot{x}_c(t)=\frac{g_1}{g_5g_7}\cdot P_a(t)+\frac{g_2}{g_6g_8}\cdot P_b(t) \tag{24}$$

$$\dot{z}_c(t)=\frac{g_3}{g_5g_7}\cdot P_a(t)+\frac{g_4}{g_6g_8}\cdot P_b(t) \tag{25}$$

Appendix J Quantization of crisp data

Table 1. Arm and boom angle error quantization levels.

Quantization level	Arm angle error, e_α [bit]	Boom angle error, e_β [bit]	Angle error [rad]	Quantized angle error [rad]
1	[91, 3 477]	[121, 3 177]	$-1.931 < e_\alpha \leqq -0.0500$ $-1.319 < e_\beta \leqq -0.0500$	−0.0500
2	[86, 90]	[115, 120]	$-0.0500 < e_\alpha, e_\beta \leqq -0.0475$	−0.0475
3	[82, 85]	[109, 114]	$-0.0475 < e_\alpha, e_\beta \leqq -0.0450$	−0.0450
4	[77, 81]	[103, 108]	$-0.0450 < e_\alpha, e_\beta \leqq -0.0425$	−0.0425
5	[73, 76]	[97, 102]	$-0.0425 < e_\alpha, e_\beta \leqq -0.0400$	−0.0400
6	[68, 72]	[91, 96]	$-0.0400 < e_\alpha, e_\beta \leqq -0.0375$	−0.0375
7	[64, 67]	[85, 90]	$-0.0375 < e_\alpha, e_\beta \leqq -0.0350$	−0.0350
8	[59, 63]	[79, 84]	$-0.0350 < e_\alpha, e_\beta \leqq -0.0325$	−0.0325
9	[55, 58]	[73, 78]	$-0.0325 < e_\alpha, e_\beta \leqq -0.0300$	−0.0300
10	[50, 54]	[67, 72]	$-0.0300 < e_\alpha, e_\beta \leqq -0.0275$	−0.0275
11	[46, 49]	[61, 66]	$-0.0275 < e_\alpha, e_\beta \leqq -0.0250$	−0.0250
12	[41, 45]	[55, 60]	$-0.0250 < e_\alpha, e_\beta \leqq -0.0225$	−0.0225
13	[37, 40]	[49, 54]	$-0.0225 < e_\alpha, e_\beta \leqq -0.0200$	−0.0200
14	[32, 36]	[43, 48]	$-0.0200 < e_\alpha, e_\beta \leqq -0.0175$	−0.0175
15	[28, 31]	[37, 42]	$-0.0175 < e_\alpha, e_\beta \leqq -0.0150$	−0.0150
16	[23, 27]	[31, 36]	$-0.0150 < e_\alpha, e_\beta \leqq -0.0125$	−0.0125
17	[19, 22]	[25, 30]	$-0.0125 < e_\alpha, e_\beta \leqq -0.0100$	−0.0100
18	[14, 18]	[19, 24]	$-0.0100 < e_\alpha, e_\beta \leqq -0.0075$	−0.0075
19	[10, 13]	[13, 18]	$-0.0075 < e_\alpha, e_\beta \leqq -0.0050$	−0.0050
20	[5, 9]	[7, 12]	$-0.0050 < e_\alpha, e_\beta \leqq -0.0025$	−0.0025
21	[−4, 4]	[−6, 6]	$-0.0025 < e_\alpha, e_\beta < 0.0025$	0.0000
22	[−9, −4]	[−12, −7]	$0.0025 \leqq e_\alpha, e_\beta < 0.0050$	0.0025
23	[−13, −10]	[−18, −13]	$0.0050 \leqq e_\alpha, e_\beta < 0.0075$	0.0050
24	[−18, −14]	[−24, −19]	$0.0075 \leqq e_\alpha, e_\beta < 0.0100$	0.0075
25	[−22, −19]	[−30, −25]	$0.0100 \leqq e_\alpha, e_\beta < 0.0125$	0.0100
26	[−27, −23]	[−36, −31]	$0.0125 \leqq e_\alpha, e_\beta < 0.0150$	0.0125
27	[−31, −28]	[−42, −37]	$0.0150 \leqq e_\alpha, e_\beta < 0.0175$	0.0150
28	[−36, −32]	[−48, −43]	$0.0175 \leqq e_\alpha, e_\beta < 0.0200$	0.0175
29	[−40, −37]	[−54, −49]	$0.0200 \leqq e_\alpha, e_\beta < 0.0225$	0.0200
30	[−45, −41]	[−60, −55]	$0.0225 \leqq e_\alpha, e_\beta < 0.0250$	0.0225
31	[−49, −46]	[−66, −61]	$0.0250 \leqq e_\alpha, e_\beta < 0.0275$	0.0250
32	[−54, −50]	[−72, −67]	$0.0275 \leqq e_\alpha, e_\beta < 0.0300$	0.0275
33	[−58, −55]	[−78, −73]	$0.0300 \leqq e_\alpha, e_\beta < 0.0325$	0.0300
34	[−63, −59]	[−84, −79]	$0.0325 \leqq e_\alpha, e_\beta < 0.0350$	0.0325
35	[−67, −64]	[−90, −85]	$0.0350 \leqq e_\alpha, e_\beta < 0.0375$	0.0350
36	[−72, −68]	[−96, −91]	$0.0375 \leqq e_\alpha, e_\beta < 0.0400$	0.0375
37	[−76, −73]	[−102, −97]	$0.0400 \leqq e_\alpha, e_\beta < 0.0425$	0.0400
38	[−81, −77]	[−108, −103]	$0.0425 \leqq e_\alpha, e_\beta < 0.0450$	0.0425

Table 1. Continued

39	[−85, −82]	[−114, −109]	$0.0450 \leqq e_\alpha, e_\beta < 0.0475$	0.0450
40	[−90, −86]	[−120, −115]	$0.0475 \leqq e_\alpha, e_\beta < 0.0500$	0.0475
41	[−3 352, −91]	[−3 177, −121]	$0.0500 \leqq e_\alpha < 1.931$ $0.0500 \leqq e_\beta < 1.319$	0.0500

Table 2. Arm and boom angle error change quantization levels

Quantization level	Arm angle error change, s_α [bit/0.28 s]	Boom angle error change, s_β [bit/0.28 s]	Angle speed [rad/s]	Quantized angle speed [rad/s]
1	[202, ∞]	[270, ∞]	$s_\alpha, s_\beta \leqq -0.400$	−0.400
2	[185, 201]	[248, 269]	$-0.400 < s_\alpha, s_\beta \leqq -0.367$	−0.367
3	[169, 184]	[225, 247]	$-0.367 < s_\alpha, s_\beta \leqq -0.333$	−0.333
4	[152, 168]	[203, 224]	$-0.333 < s_\alpha, s_\beta \leqq -0.300$	−0.300
5	[135, 151]	[180, 202]	$-0.300 < s_\alpha, s_\beta \leqq -0.267$	−0.267
6	[118, 134]	[158, 179]	$-0.267 < s_\alpha, s_\beta \leqq -0.233$	−0.233
7	[102, 117]	[135, 157]	$-0.233 < s_\alpha, s_\beta \leqq -0.200$	−0.200
8	[85, 101]	[113, 134]	$-0.200 < s_\alpha, s_\beta \leqq -0.167$	−0.167
9	[68, 84]	[90, 112]	$-0.167 < s_\alpha, s_\beta \leqq -0.133$	−0.133
10	[51, 67]	[68, 89]	$-0.133 < s_\alpha, s_\beta \leqq -0.100$	−0.100
11	[34, 50]	[45, 67]	$-0.100 < s_\alpha, s_\beta \leqq -0.067$	−0.067
12	[17, 33]	[23, 44]	$-0.0667 < s_\alpha, s_\beta \leqq -0.033$	−0.033
13	[−16, 16]	[−22, 22]	$-0.0333 < s_\alpha, s_\beta < 0.033$	0.000
14	[−33, −17]	[−44, −23]	$0.033 \leqq s_\alpha, s_\beta < 0.067$	0.033
15	[−50, −34]	[−67, −45]	$0.067 \leqq s_\alpha, s_\beta < 0.100$	0.067
16	[−67, −51]	[−89, −68]	$0.100 \leqq s_\alpha, s_\beta < 0.133$	0.100
17	[−84, −68]	[−112, −90]	$0.133 \leqq s_\alpha, s_\beta < 0.167$	0.133
18	[−101, −85]	[−134, −113]	$0.167 \leqq s_\alpha, s_\beta < 0.200$	0.167
19	[−117, −102]	[−157, −135]	$0.200 \leqq s_\alpha, s_\beta < 0.233$	0.200
20	[−134, −118]	[−179, −158]	$0.233 \leqq s_\alpha, s_\beta < 0.267$	0.233
21	[−151, −135]	[−202, −180]	$0.267 \leqq s_\alpha, s_\beta < 0.300$	0.267
22	[−168, −152]	[−224, −203]	$0.300 \leqq s_\alpha, s_\beta < 0.333$	0.300
23	[−184, −169]	[−247, −225]	$0.333 \leqq s_\alpha, s_\beta < 0.367$	0.333
24	[−201, −185]	[−269, −248]	$0.367 \leqq s_\alpha, s_\beta < 0.400$	0.367
25	[−∞, −202]	[−∞, −270]	$0.400 \leqq s_\alpha, s_\beta$	0.400

Table 3. Arm and boom cylinder control quantization levels when field tuning tactor is 2.2

Quantization level	FLC output [Volt]	Quantized control output [Volt]	Arm and boom cylinder control, c_α and c_β [bit]	PIO output ON=1, OFF=0
1	$c_\alpha, c_\beta \leqq -0.364$	−2.5	2 047	0
2	$-0.363 \leqq c_\alpha, c_\beta \leqq -0.319$	−2.4	1 965	0
3	$-0.318 \leqq c_\alpha, c_\beta \leqq -0.273$	−2.3	1 883	0
4	$-0.272 \leqq c_\alpha, c_\beta \leqq -0.228$	−2.2	1 801	0
5	$-0.227 \leqq c_\alpha, c_\beta \leqq -0.182$	−2.1	1 719	0
6	$-0.181 \leqq c_\alpha, c_\beta \leqq -0.137$	−2.0	1 638	0
7	$-0.136 \leqq c_\alpha, c_\beta \leqq -0.091$	−1.9	1 556	0
8	$-0.090 \leqq c_\alpha, c_\beta \leqq -0.046$	−1.8	1 474	0
9	$-0.045 \leqq c_\alpha, c_\beta \leqq -0.000$	−1.7	1 392	0
10	$0.000 \leqq c_\alpha, c_\beta \leqq 0.045$	1.7	1 392	1
11	$0.046 \leqq c_\alpha, c_\beta \leqq 0.090$	1.8	1 474	1
12	$0.091 \leqq c_\alpha, c_\beta \leqq 0.136$	1.9	1 556	1
13	$0.137 \leqq c_\alpha, c_\beta \leqq 0.181$	2.0	1 638	1
14	$0.182 \leqq c_\alpha, c_\beta \leqq 0.227$	2.1	1 719	1
15	$0.228 \leqq c_\alpha, c_\beta \leqq 0.272$	2.2	1 801	1
16	$0.273 \leqq c_\alpha, c_\beta \leqq 0.318$	2.3	1 883	1
17	$0.319 \leqq c_\alpha, c_\beta \leqq 0.363$	2.4	1 965	1
18	$c_\alpha, c_\beta \geqq 0.364$	2.5	2 047	1